THE INVESTIGATIONS ON THE MODIFIED Y-ZEOLITE BASED FCC CATALYST: EFFECT OF ZEOLITE TO MATRIX RATIO

BY

ADEEL AHMAD

A Thesis Presented to the

DEANSHIP OF GRADUATE STUDIES

KING FAHD UNIVERSITY OF PETROLEUM & MINERALS

DHAHRAN, SAUDI ARABIA

In Partial Fulfillment of the
Requirements for the Degree of

MASTER OF SCIENCE

CHEMICAL ENGINEERING

DECEMBER 2020

KING FAHD UNIVERSITY OF PETROLEUM & MINERALS

DHAHRAN- 31261, SAUDI ARABIA

DEANSHIP OF GRADUATE STUDIES

This thesis, written by **ADEEL AHMAD** under the direction of his thesis advisor and approved by his thesis committee, has been presented and accepted by the Dean of Graduate Studies, in partial fulfilment of the requirements for the degree of **MASTER OF SCIENCE IN CHEMICAL ENGINEERING.**

Dr. Abdallah Al-Shammari
(Advisor)

Dr. Mamdouh Al-Harthi
Department Chairman

Dr. Shakeel Ahmed
(Co-Advisor)

Dr. Hassan Saeed Alasiri
(Member)

Dr. Suliman Saleh Al-Homidan
Dean of Graduate Studies

Dr. Mohammad M. Hossain
(Member)

Date

Dr. Shaikh Abdur Razzak
(Member)

Dedicated to Almighty ALLAH and my beloved parents

ACKNOWLEDGEMENTS

Praise be to Allah almighty, Lord of the Universe.

I am forever indebted to Allah almighty for blessing me with all the good things in my life. I am grateful to my parents who have nurtured me and made me the responsible man that I am today. My wife is a huge part of my professional struggle and her constant support and affection for me made challenges easy for me. My beloved kids have also helped me, by just being the lovely kids that they are.

I would like to thank my advisor Dr Abdallah Al-Shammari who has been my advisor and mentor in my M.Sc. program. He has constantly guided me and helped me in my academic and administrative issues. He always found time for me in his busy schedule and gave feedback to me from time to time regarding my thesis work.

I express my gratitude to my co-advisor Dr Shakeel Ahmed who helped me in my experimental work. He solved my technical problems and assisted me with my work. I am also grateful to my committee members Dr Hassan Saeed Alasiri, Dr Mohammed Mozahar Hossain and Dr. Shaikh Abdur Razzak for their valuable feedback, their insightful comments and valuable suggestions. I would also appreciate Engr. Rahat Saeed and Engr. Abdul Bari for training me on the MAT unit and the assistance from Mr Reynante.

Lastly, I am thankful to all my friends here who have made my stay enjoyable and memorable. I am indeed very grateful.

TABLE OF CONTENTS

LIST OF TABLES

LIST OF FIGURES

LIST OF ABBREVIATIONS

FCC	:	Fluid Catalytic Cracking
VGO	:	vacuum Gas Oil
ECAT	:	Equilibrium Catalyst
MAT	:	Micro Activity Testing
CTAB	:	Cetyltrimethylammonium Bromide
USY	:	Ultra Stable Y-zeolite
TOS	:	Time on stream
LCO	:	Light Cycle Oil
HCO	:	Heavy Cycle Oil
St	:	Steamed
MY	:	Modified Y-zeolite

ABSTRACT

Full Name : Adeel Ahmad

Thesis Title : The investigations on the modified Y-zeolite based FCC catalyst: Effect of Zeolite to Matrix ratio

Major Field : Chemical Engineering

Date of Degree : December 2020

A wide range of processes and reactions in the industry have utilized zeolites as well as relevant crystalline molecular sieves due to their microporous structure, shape selectivity, ion exchange capability, and strong acidity. The small size of cavities and narrow channels inside Y-zeolite impedes their practical applications, and therefore, several studies have been conducted to accommodate the transportation of heavy molecules in the micropore. This study focuses on the generation of mesoporosity inside Y-zeolite, by post-treatment of commercial Y-Zeolite with acid, base, and organic template cetyltrimethylammonium bromide (CTAB). Modified Y-zeolites were used for the preparation of FCC catalysts. FCC catalysts consisted of a modified Y-zeolite and amorphous matrix. The matrix was composed of amorphous silica-alumina, kaolin, and silica sol binder. The FCC catalysts were steamed at 750 °C for 5hr to measure the hydrothermal stability. Performance evaluation of the catalysts was calculated at 550 °C to see the yield of gasoline, LCO, HCO, and coke. Vacuum gas oil (VGO) was used as feed for testing of FCC catalyst in fixed bed micro activity test (MAT) unit. A series of five FCC catalysts using Ultra-stable Y-zeolite was prepared with Zeolite to matrix ratio varying from 18 to 50, to obtain a base catalyst for comparison with modified Y-zeolite-based FCC catalyst. The effect of Zeolite to matrix

ratio on product yield (%) from VGO cracking has been studied. Modified Y-zeolite and as-synthesized FCC catalysts were characterized by using XRD, N_2 adsorption isotherm, ICP, NH_3-TPD and SEM analysis to measure their physical and chemical properties. A comparison of modified Y-zeolite based FCC catalysts with USY based FCC catalyst for zeolite to matrix ratio of 18 has been carried out. Modified Y-zeolite based FCC catalysts gives significant enhancement in product selectivity as compared to USY based FCC catalyst due to reduced diffusion limitations of reactants as well as products. The relative difference in gasoline selectivity of modified Y-zeolite based FCC catalysts (St-MY02 & St-MY03) was +3.4% and +1.7% respectively, whereas -14.4% and -1.4% was noted as a relative difference of coke selectivity as compared to the base catalyst (St-Y01).

ملخص الرسالة

الاسم الكامل : عديل احمد

عنوان الرسالة : **التحقيقات حول محفز التكسير التحفيزي المائع المعتمد على Y- زيوليت: تأثير نسبة الزيوليت إلى نسبة المصفوف**

التخصص : **هندسة كيميائية**

تاريخ الدرجة العلمية : ديسمبر 2020

استخدمت مجموعة واسعة من العمليات والتفاعلات في الصناعة الزيوليت وكذلك المناخل الجزيئية البلورية ذات الصلة بسبب هيكلها الصغير الذي يسهل اختراقه وانتقائية الشكل والقدرة على التبادل الأيوني والحموضة القوية. يعيق صغر حجم التجاويف والقنوات الضيقة داخل Y-zeolite تطبيقاتها العملية ، وبالتالي ، تم إجراء العديد من الدراسات لاستيعاب نقل الجزيئات الثقيلة في المسام الصغير. تركز هذه الدراسة على توليد اللزوجة المتوسطة داخل Y-zeolite ، عن طريق المعالجة اللاحقة لـ Y-Zeolite التجارية باستخدام قالب سيتيل ترايميثيل الأمونيوم الحمضي والقاعدة والعضوية (CTAB). تم استخدام زيوليت Y المعدلة لتحضير محفزات التكسير التحفيزي المائع. تتكون محفزات التكسير التحفيزي المائع من مصفوفة Y- زيوليت معدلة وغير متبلورة. كانت المصفوفة مكونة من سيليكا-ألومينا غير متبلورة ، كاولين ، وسيليكا سول الموثق. تم تبخير محفزات التكسير التحفيزي المائي عند 750 درجة مئوية لمدة 5 ساعات لقياس الاستقرار الحراري المائي. تم حساب تقييم أداء المحفزات عند 550 درجة مئوية لمعرفة محصول البنزين و LCO و HCO وفحم الكوك. تم استخدام زيت الغاز الفراغي (VGO) كغذاء لاختبار محفز التكسير التحفيزي المائع في وحدة اختبار النشاط الجزئي ذات القاعدة الثابتة (MAT). تم تحضير سلسلة من خمسة محفزات التكسير التحفيزي المائع باستخدام زيوليت Y فائق الثبات مع نسبة زيوليت إلى مادة أساس تتراوح من 18 إلى 50 ، للحصول على محفز أساسي للمقارنة مع محفز التكسير التحفيزي المائع القائم على Y- زيوليت. تمت دراسة تأثير نسبة الزيوليت إلى مادة الأساس على إنتاجية المنتج (٪) من تكسير VGO. تم وصف محفزات Y-zeolite المعدلة ومحفزات FCC كمركبة باستخدام XRD و N2 متساوي حرارة الامتزاز و ICP و NH3-TPD و SEM لقياس خواصها الفيزيائية والكيميائية. تم إجراء مقارنة بين محفزات التكسير التحفيزي المائع المعتمد على Y- زيوليت مع محفز FCC المعتمد على USY للزيوليت إلى نسبة المصفوفة 18. تعطي محفزات التكسير التحفيزي المائع المعتمد

على Y- زيوليت تحسينًا كبيرًا في انتقائية المنتج مقارنة بمحفز FCC المعتمد على USY بسبب قيود الانتشار المنخفضة للمواد المتفاعلة وكذلك المنتجات. كان الاختلاف النسبي في انتقائية البنزين لمحفزات التكسير التحفيزي المائع المعتمد على Y- زيوليت (St-MY02 & St-MY03) + 3.4٪ و + 1.7٪ على التوالي ، بينما لوحظ -14.4٪ و -1.4٪ على أنهما فرق نسبي لانتقائية فحم الكوك بالمقارنة مع المحفز الأساسي (St-Y01).

CHAPTER 1

INTRODUCTION

1.1 Background

The heavy fractions of petroleum hydrocarbons were cracked into light fractions originally done by thermal cracking. Later, it was replaced by FCC process due to the enhancement of gasoline yield with a high-octane rating. The by-product gases produced by FCC are more olefinic and valuable as compared to thermal cracking [1].

The fluid catalytic cracking process used in oil and gas industries as a conversion technology to produce a major part of the gasoline. FCC is not only the single process used in oil and gas industries for the conversion, but hydrocracking is also used for the same purposes. Even though the fluid catalytic field has been studied already for 75 years but still this area is central as a research point of view for both the industry and academia [2]. FCC process is operational across the globe in 300 refineries out of 646 in total since 2014 [3]. FCC catalyst production is estimated at 840,000 metric tons per year. It is estimated that 0.16 kg of FCC catalyst is used per barrel of feedstock (vacuum gas oil). For heavy feed materials, such as resid, 0.20 kg of FCC catalyst is used per barrel [4].

Daily used globally transportation fuels i.e., jet fuels, diesel and gasoline are the most valuable products. Our primary objective is the extraction of these products from crude oil at affordable prices with less environmental pollution. Therefore, efforts have been employed to develop new technologies [5-8].

In FCC, the choice of the most suitable catalyst is very crucial for the success of a process as a result of a high gasoline yield. Although, there are different zeolite-based catalysts are tested but less yield of the desired products, huge energy requirements for the process and poor stability of the catalyst at elevated temperatures lead towards the better catalyst design suitable for the catalytic process [9-11]. Y-zeolite is considered a primary cracking component in the FCC catalyst since 1964 [12]. ZSM-5, which was invented in 1973 is used as a second FCC catalyst. It has the main application in the enhancement of the propylene yield [13]. The addition of zeolite materials in the FCC catalyst field has led to a significant enhancement of the gasoline yield [14].

Zeolite crystals with some unique characteristics such as shape selectivity, high surface area as well as acidity had wide applications in industry as a heterogeneous catalyst. It is widely used in solid acid-catalyzed reactions in the oil and gas industry as well as the petrochemical sector [15]. Due to their small pore size (<1.5nm), zeolite crystals often find slow diffusion of heavy molecules specifically in area of fine chemicals as well as upgrading of vacuum gas oil or residue [16-19]. But severe restriction of diffusion due to the microporous structure of zeolite impedes their use in reactions involving heavy molecules [20]. In most of the industrially used nano porous materials, Y-zeolite (0.74 nm pore diameter) has significant importance in catalysis due to its advantageous features such as high acid strength, activity, shape selectivity, and stability at high temperature [21-23].

The addition of a Nanosized pore network inside the zeolite may help to reduce the diffusion limitation problem. Thus, hierarchal zeolite synthesis seeks attraction among materials as well as catalysis researchers. Certain promising techniques have been applied for the hierarchical porous zeolite, mostly were mesoporous zeolites. The approaches used

to create the mesoporosity are as follows: (1) Dematalization includes dealumination and desilication [24, 25]which involves post-synthetic treatment to create the mesoporosity (2) framework crystallization of synthesized mesoporous aluminosilicates [25, 26] using the steam aided methods of crystallization (3) Assembly of nanosized zeolite crystals in which mesoporosity generated inside the Zeolites [27]. Some of these methods are limited by high cost, partial destruction in zeolite structure, extra framework aluminum species formation, and uneven mesoporosity generated by the treatment [28, 29]. Some of the hierarchical zeolites i.e., faujasite, ZSM-5, as well as mordenite were obtained successfully by post-treatment methods in the presence of acid and base along with surfactant [30-32]. These materials have much improved acidity as well as hydrothermal stability. One thing important is that there is a connection between intracrystalline mesopore formation as well as zeolite micropore size. It is suggested that 12-membered ring pores present in faujasite are reachable by the surfactant species which facilitates the generation of long-range mesopores during the surfactant-based mesostructuring process. On the other hand, 10-membered ring channels of ZSM-5 would be out of reach for the surfactant. Therefore, no long range mesoporosity would be observed in modified zeolite [33]. A method that can generate controlled mesoporosity inside crystalline structure of zeolite considered to be highly useful and created a huge effect on catalytic side like in FCC process [34]. A series of parent and hierarchical zeolite i.e., Y-zeolite as well as ZSM-5 were modified with acid, base, and surfactant template method. The effect of gasoline and propylene yield was significant as compared to conventional zeolites [35].

In general, the modern FCC catalyst comprises of two components: zeolite and a matrix. Ternary component can be added in FCC catalyst as an additive to increase metal resistance

in a catalyst, boost octane number of gasoline or reduce the emissions of SO_x. Most FCC catalysts contain 15 to 45% of zeolite which contributes majorly to selectivity and catalytic activity in FCC catalytic reactions [36]. It was observed that olefin to paraffin ratio decreases with the increase of zeolite content in FCC catalysts due to the higher hydrogen transfer reaction rate [37]. Commercially available FCC catalysts are prepared by using zeolites dispersed in a silica-alumina matrix to form 60μm particle size [38]. The FCC catalyst consists of 60 to 85% by weight of matrix which contains natural as well as synthetic components [39]. An active matrix holds acidic sites because of the presence of alumina. On the other hand, inactive matrix does not influence the catalytic performance of FCC catalyst due to the absence of acidic sites [40]. Zeolite properties have more effect on the cracking products like gas and gasoline, whereas the matrix only has a direct effect on heavier light cycle oil (LCO). The chemical composition of zeolite and matrix creates a considerable effect in FCC selectivity [41]. The most important function of matrix is pre-cracking the FCC resid and decrease the direct contact of cracked products to highly acid sites of the Y-Zeolite. Afterward, pre-cracked products are diffused easily into the zeolite pores to crack further on strong acidic sites of a Zeolite [42, 43]. Steaming is considered one of the essential steps in the utilization and activation of FCC catalysts. Some of the zeolites are destroyed during steaming because of the dealumination of framework of the Y-zeolite. Hydrothermal treatment of the FCC catalyst is used to replicate the deactivation that happens in a commercial unit to form an equilibrium catalyst. FCC catalyst steaming leads towards the actual evaluation of the catalyst because the catalyst activity in its fresh state cannot give the exact idea of its commercial performance. The temperature used for the hydrothermal pre-treatment of fresh FCC catalysts is varied from 538-927 °C during a

time period of 2-24h in the presence of 100% steam. The selectivity as well as activity of FCC catalyst are altered depending on the steaming conditions. Therefore, in commercial FCC unit, the equilibrium catalyst gives a different yield of products as compared to fresh catalyst [44, 45]. Prepared catalysts could be evaluated in a MAT (micro activity test) unit on vacuum gas oil (VGO) feed. All MAT test has to be run at 550ºC temperature and time on stream (TOS) 30sec [46].

1.2 Objectives

The purpose of this study is to investigate the effects of the preparation of modified Y-zeolite based FCC catalysts on the enhancement of gasoline selectivity as well as a reduction in coke selectivity. Further, the effect of zeolite to matrix ratio on product selectivity after VGO cracking has been also studied for USY based FCC catalysts.

The specific objectives of this research work are:

- Mesoporosity generation in conventional Y-zeolite to reduce diffusion limitations of heavy FCC feed molecules
- Study the effect of modified Y-zeolite based FCC on VGO cracking
- Study the effect of Zeolite to Matrix ratio using USY zeolite on VGO cracking
- Characterization of modification Y-zeolite and FCC catalysts
- Performance evaluation of FCC catalysts in MAT unit

CHAPTER 2

LITERATURE REVIEW

2.1 Fluid catalytic cracking

FCC process is used in most oil and gas industries to convert low-value hydrocarbons such as heavy gas oil, residue, and vacuum gas oil into high value products i.e., gasoline and light olefinic gases.

FCC feedstock usually has boiling point of 340 °C or more at atmospheric pressure as well as average molecular weight lies between 200 to 600. There is used a powdered fluidized catalyst to break the high molecules into shorter molecules by contacting the feed. In an FCC reactor, the temperature and pressure conditions are 550 °C and 1.72 bar gauge respectively. In short, FCC process is mostly fulfilling the imbalance of the market demand of gasoline products, excess of the high boiling, and heavy ends from the crude oil distillation [2].

From Figure 2.1, we can see the major difference in the yield of gases C_2-C_4, gasoline, and middle distillate before and after the FCC process. With the introduction of FCC, the yield of the high-value product has been significantly increased. Approximately 45% of the feedstock, which is naphtha, middle distillate, and C_2 to C_4 molecular range can be used further without conversion.

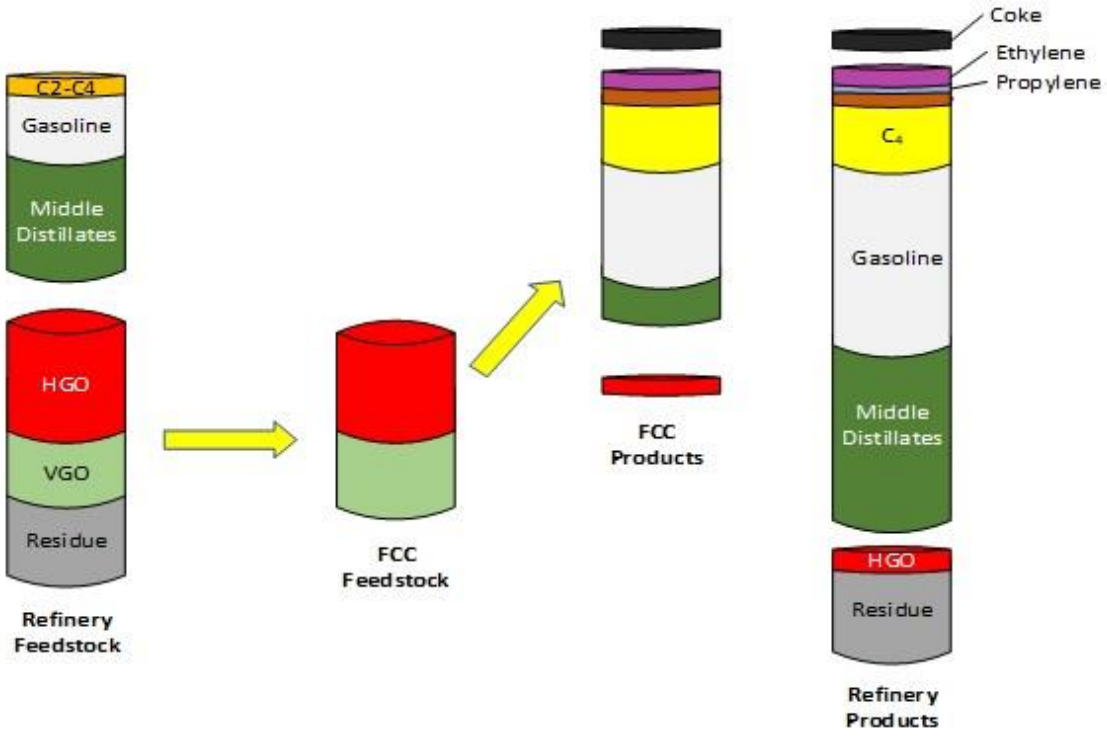

Figure 2.1: Effect of FCC conversion on refinery products [47].

But isomerization as well as reforming needs to be increased the value of the products. Moreover, hydrotreating has to be done to remove the amount of sulfur before used in vehicles to avoid environmental hazards [47].

2.2 Fluid catalytic cracking catalyst material

2.2.1 Structure and composition

Some desirable properties should be present inside the fluid catalytic cracking catalyst to make it perfect for the cracking of heavier hydrocarbons. The desirable characteristics of an FCC catalyst are:

Activity and selectivity: It should be present in FCC catalyst to convert the heavy hydrocarbons into valuable products.

Hydrothermal stability: A Fluid catalytic cracking catalyst should be able to resist high temperatures as well as steam partial pressure used for better efficiency in the regenerator.

Metals tolerance: Some metals in fluid catalytic cracking feed acts as poisons for the catalyst. So, it has enough tolerance to negate the effect of metals.

Attrition resistance: Particles of catalyst must withstand the impacts with the wall during the circulation as well as each other also.

Coke selectivity: Less coke should be deposited on FCC catalyst during the processing of heavier hydrocarbons especially in case of resids for the better yield of gasoline.

Fluidizability: Components of catalyst should be present in the form that permits fluidization on the regenerator [14].

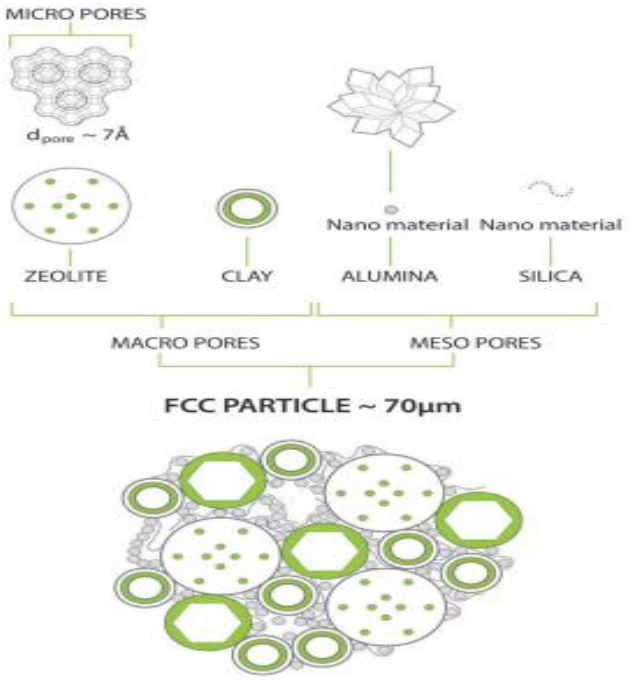

Figure 2.2: Typical structural and chemical composition of a FCC catalyst [13].

All demands mentioned above could be found in one catalytic material that combines the number of components as shown in Figure 2.2. The main active component of FCC catalyst is usually Y-zeolite in the stabilized form. This catalytic material consisted of internal pores that contain active acid sites present inside due to which heavy hydrocarbons converted into gasoline yield. Clay is used as a filler as well as heat capacity reasons. Many sources of silica as well as alumina are used to make a meso-macroporous FCC matrix that pre-cracks the larger feed molecules. Moreover, these components impart physical strength and integrity to the system. Additional components are used to traps the metal components like Ni and V. The components of the FCC matrix are usually mixed in the form of aqueous slurry. The spray drying method is used to make spherical shape particles of catalysts that are easily fluidized in the regenerator [14].

2.2.2 Reactions

The cracking reactions are the combination of thermal as well as catalytic reactions, where catalytic reactions are more important. During the reactions, pre-cracking of the large molecules takes place in the amorphous silica-alumina matrix before entering into the micropores of the zeolite.

In Figure 2.3, we can see the simple overview of the FCC cracking reactions from feedstock to the gasoline and gaseous products. We can see that conversion has occurred in different steps where gasoline is not only the primary reaction product [48].

The cracking reactions are acid-catalyzed. Although the mechanism of catalytic cracking has already been described from the early stages of catalytic cracking. Therefore, this thing is obvious that Carbenium ions formed during catalytic reactions [49, 50].

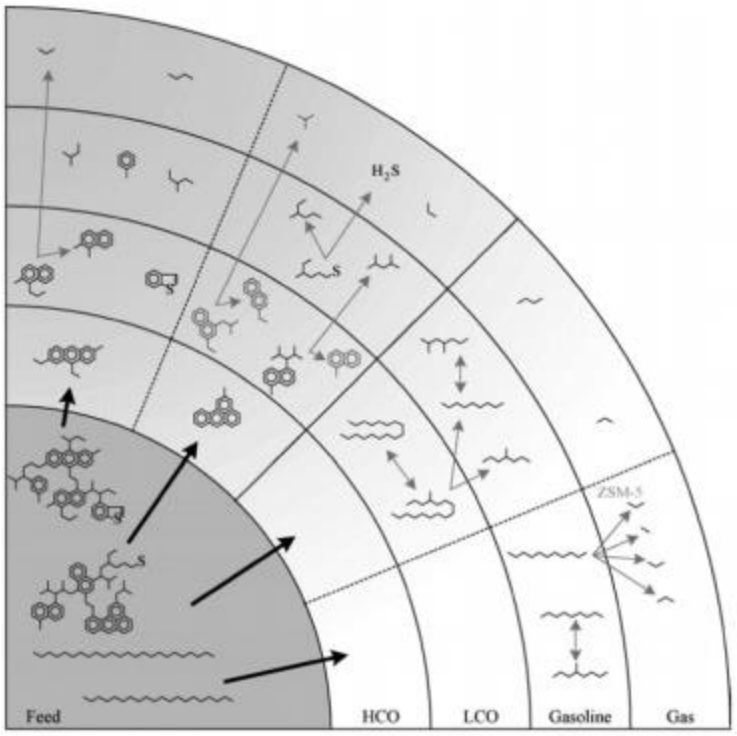

Figure 2.3: Series of cracking reactions of heavier feedstock leads to the FCC products [46].

From Figure 2.4, we can see the four reactions occurred to form the carbenium ion. In a reaction 1, carbenium ion has been formed by the transfer of a proton from Bronsted zeolite site to the alkane and in reaction 2, proton transfer towards the alkene molecule. But in reaction 3, the formation of carbenium ion by the transfer of proton towards alkane from Zeolite, and in reaction 4, alkene and new carbenium ion formation takes place by the beta scission of a carbenium ion [51, 52].

It is concluded that formation of initially formed carbenium ion on Lewis and Bronsted sites occurred in parallel in both pathways [49].

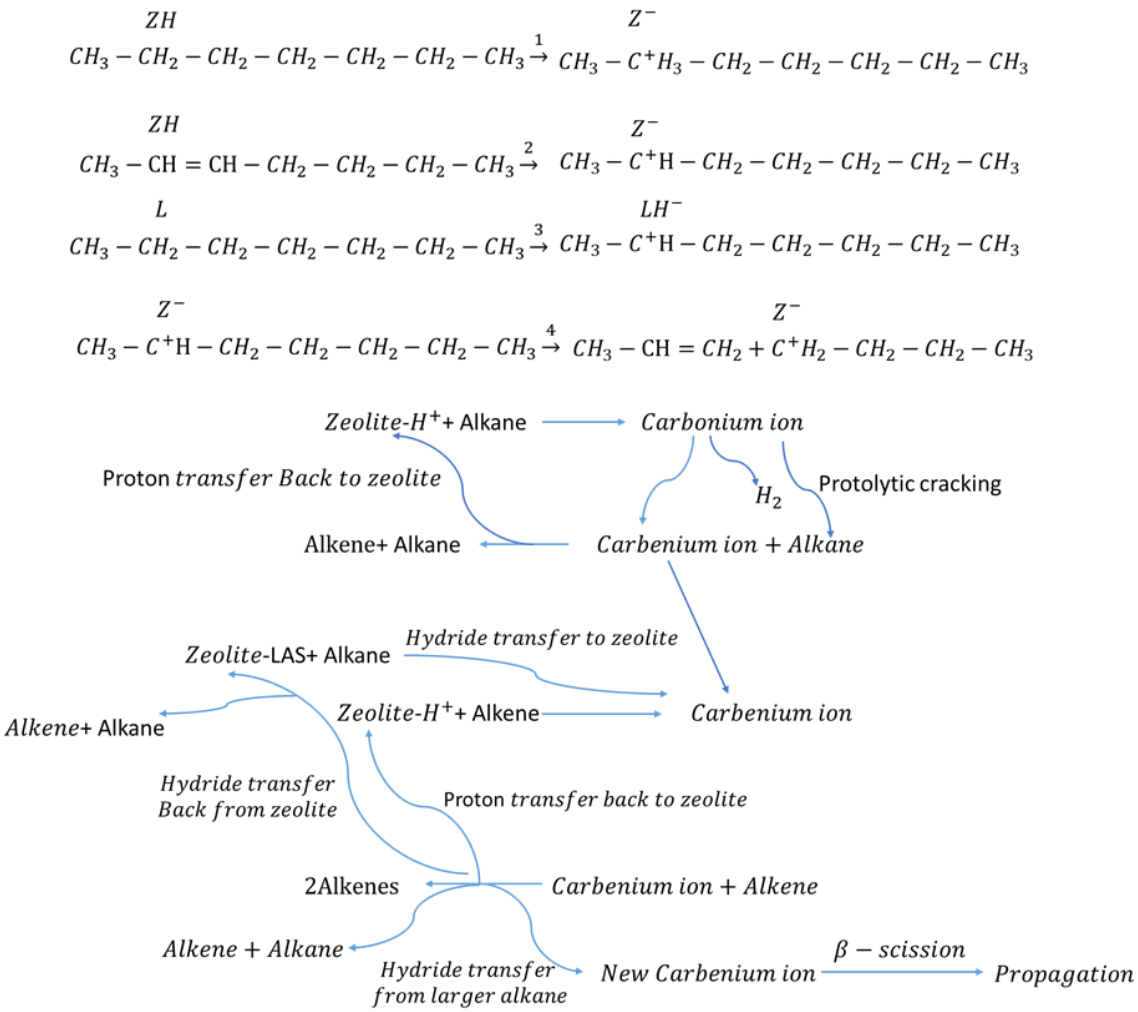

Figure 2.4: Mechanism of hydrocarbons cracking reaction network on zeolite [49, 50].

2.3 Hierarchical zeolites

Zeolites are sometimes called molecular sieves that are crystalline aluminosilicates of alkaline elements that display some unique properties in the field of catalysis [53]. Although there are numerous advantages of using zeolites, diffusion limitation for branched molecules as well as the transfer of molecules with a size similar to the micropore creates difficulty for its further use in the conversion of heavy molecules [19]. Diffusion limitation facilitates the conversion of molecules into by-products which are undesirable

due to consisting of coke precursors. These coke precursors can block the micropores of the catalyst which causes the deactivation of a catalyst and reduce the life span of a catalyst as well.

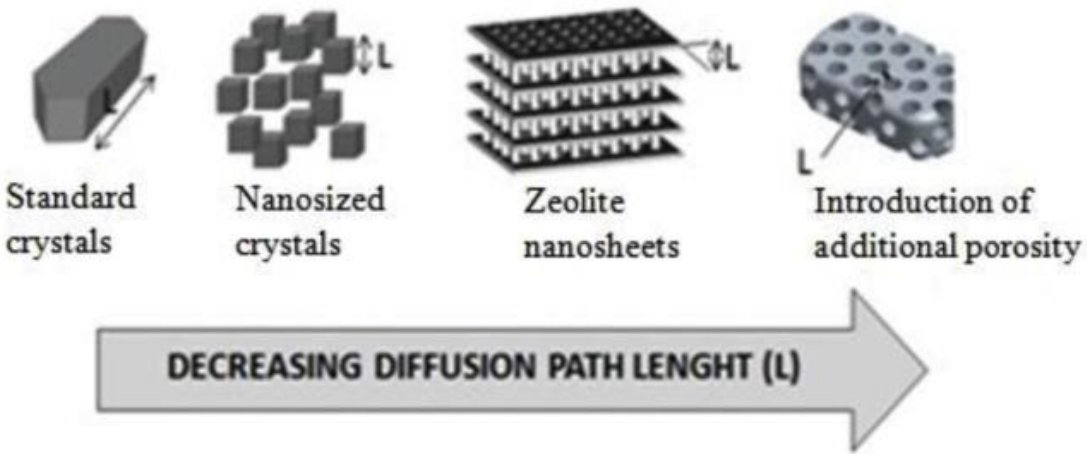

Figure 2.5: Effect of crystals on diffusion path length [52].

In this kind of situation, the only external surface area of the catalyst used while the internal surface area remains inactive. However, efforts have started on the hierarchical zeolite synthesis which has secondary porosity in the mesopore range (2 to 50 nm pore size). Such solution provides ease to the approach of heavy molecules towards the active centers of the catalyst while maintaining the crystallinity as well as the acidity of zeolites simultaneously [54].

From Figure 2.5, we can see the effect of crystals shape and size on the diffusion path length during the reaction on the catalyst surface. We can see additional porosity decreases the diffusion limitation the same as in the case of mesoporous zeolites.

However, creating additional porosity in zeolites is a challenge for scientists. Several methods have already been introduced for the preparation of hierarchical zeolite, but care must be taken to create secondary porosity without the detriment of the micropores structure to make it effective for further use.

2.4 Methods of synthesis of hierarchical zeolites

There are certain methods of hierarchical zeolite synthesis to create secondary porosity. Here are two approaches which renowned for these purposes are:

1. Top-down approach
2. Bottom-up approach

These two approaches have been classified into further types of producing hierarchical zeolite [55].

Top-down approach

- Dealumination
- Desilication
- Irradiation
- Surfactant templated recrystallization

Bottom-up approach

- Hard templating method
- Soft templating method
- Assembly of nanosized zeolites
- Zeolitization of materials

2.4.1 Dealumination

Dealumination is a method to create mesoporosity by leaching the aluminum ion from the zeolite structure by using the hydrothermal treatment or the chemical reagents [56]. The extraction of aluminum with the help of acid at elevated temperature is the most commonly used technique that was first described in 1960 by Barrer [57].

The formation of vacancies is created by the elution of aluminum with a partial breakdown of the crystalline structure of the zeolite. The vacancies consist of second porosity in the range of mesopore in the micropore zeolite structure. However, it is noticed that dealumination causes a drastic effect on the acidic nature of the zeolite which depends on the method used [58].

Aluminum species were removed in the reaction of zeolite with hydrochloric acid to enhance the Si/Al ratio. There is discussed a dealumination method in the presence of hydrochloric acid in literature with the following steps [59]:

- At 140°C temperature, synthesis, and aging of the solution having nanoparticles of zeolite
- Gradual cooling at room temperature
- Acidification by using concentrated hydrochloric acid
- Hydrothermal treatment at 150°C for 75h

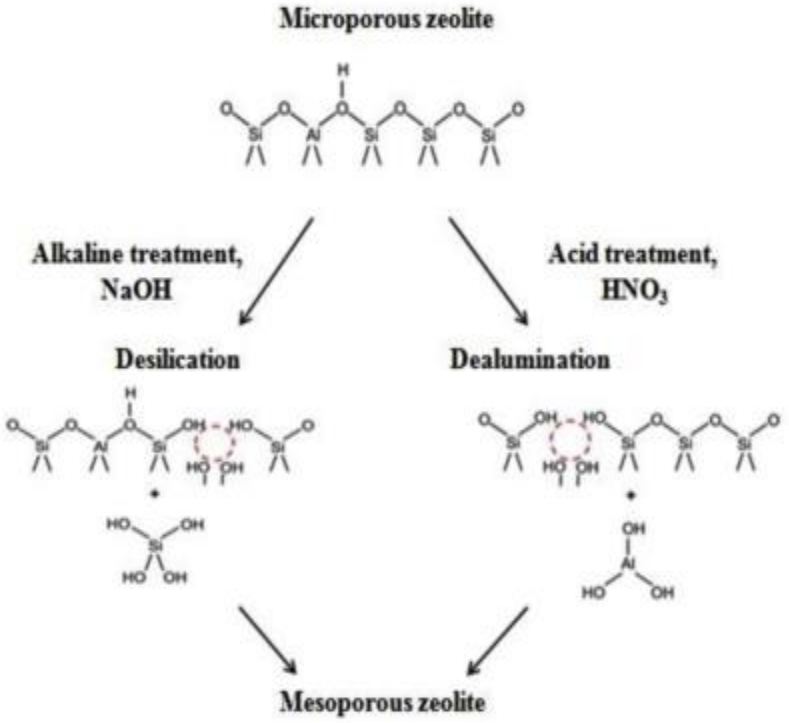

Figure 2.6: Dealumination and Desilication method [58].

Dealumination creates a loss of crystallinity of framework and fewer acid sites. Hence, these drawbacks are more than offset by the enhanced diffusional properties and the creation of new acidic sites [60]. Dealumination considers a low-cost method to create the mesoporosity in Y-zeolite in post-treatment methods. Al and Si defects created by acid washing have been studied in Y zeolite framework during dealumination [61].

2.4.2 Desilication

This method is used to create mesoporosity by the removal of Si from the zeolite structure in an alkaline medium. Hierarchical zeolite obtained by this method is acknowledged by the presence of 2nd porosity simultaneously maintaining the structural as well as acidic

properties. Hierarchical zeolite has some new properties which affect the selectivity, activity as well as the life span of the zeolite [62].

Ogura and co-workers were the first authors who used the desilication method first time on ZSM-5. They observed the loss in microporous volume from 0.177cm3/g to 0.133cm^3/g in an alkaline environment. Moreover, increase in mesoporosity was observed from 0.072cm^3/g to 0.279cm^3/g [63].

It observed that the optimum conc. of alkali (NaOH) for the huge quantity of mesopores (>0.150cm^3/g) without affecting the crystallinity of the material was 0.2M for a time of 30 to 120 sec. At the same time, a high concentration of sodium hydroxide >1M affects the crystallinity of the material [64].

During the use of the desilication method, it happens a preferential removal of silicon from the zeolite. Mesopore surface area was approximately 200 m^2/g observed for a (Si/Al=25-50) atomic ratio after desilication. The pore size of 9 to 10 nm was observed for the atomic ratio of 25 to 50 (Si/Al). With the increase of this ratio, the size increased from 20 to 50 nm. High aluminum content retards the silicon removal for Si/Al ratio <25-50 which causes less porosity generation. In medium Si/Al ratio 25 to 50, controlled silicon removal has been observed which generates the high mesoporosity while high Si/Al > 50 creates bigger mesoporosity as well as reduces the mesopore surface. Therefore, the desilication method should be used with care to impart the additional mesoporosity along with the prevention of micropore volume loss. To that end, we can use the tertiary butyl ammonium hydroxide (TBAOH) or tertiary propyl ammonium hydroxide (TPAOH) instead of sodium hydroxide (NaOH).

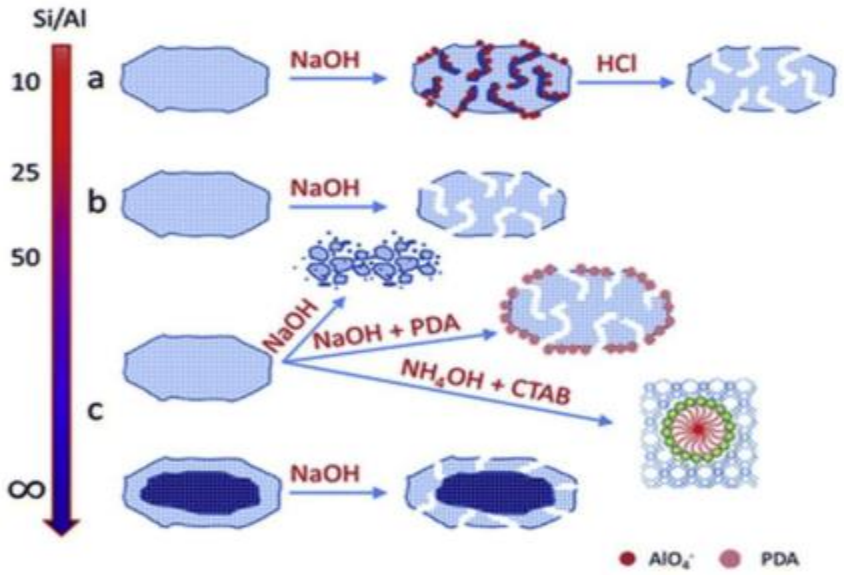

Figure 2.7: Desilication method [62].

Desilication cannot easily create perfect mesoporosity without the detriment of crystalline-acidic properties of the parent material. Therefore, a shift to the organic basis became relevant [64]. Recently, a new post-treatment method combines the alkaline hydrothermal treatment and microwave-assisted dealumination. Their effect on catalysis application has already been studied which highlighted the presence of mesoporosity inside the zeolite [65]. Further, the template-free method also applied where zirconia (Zr) atom under hydrothermal conditions applied in USY to create the mesoporosity [66]. Recently, Sn atoms are also employed in the Y-zeolite structure to enhance the mesopore volume. It is noted that the molecule (1,3,5-triisopropylbenzene) used for Catalytic cracking gives a significant enhancement in gasoline yield and lower coke tendency as compared to USY [67].

2.4.3 Irradiation

This method took place in two stages. In first stage, zeolite crystals are radiated in the presence of heavy uranium ions U^{238} to add a hidden path into the zeolite crystals. In the second step, radiated zeolite has been washed with a hydrogen fluoride solution (HF) and then water. As a result, zeolite crystals with uniform macropores in the size of 50nm have been obtained. ZSM-5 having a crystal size (5 micrometers) grow in fluoride environment have been used [68].

There is a major drawback of using the top-down approach because silica or alumina is leach away with the product streams during the desilication and dealumination [69].

2.4.4 Surfactant templated recrystallization

In 2004, a first patent application was filed to generate mesoporosity inside zeolites by using surfactant templated method and it has been mentioned also in a recent publication [70, 71]. Significantly milder conditions (dilute NH_4OH) have been used in this approach as compared to desilication. Cetyl trimethyl chloride or bromide is used as a surfactant to introduce well-controlled mesoporosity inside many zeolites i.e., ZSM-5, Mordenite, or Y-zeolite. This approach has fewer drawbacks as compared to desilication method, i.e., damage of zeolite crystals as well as the loss of silica. The original method described the modification of USY zeolite (Si/Al=15), with a solution of CTAB in 0.37 M NH_4OH or 0.09 tetrapropyl ammonium hydroxide (TPAOH) for 10 to 20 hours at 150^{o}C. Then, the surfactant (CTAB) templates were removed by calcination having a nitrogen environment, then exposed in air for uniformly distributed intractrystalline mesoporosity. A crystal rearrangement mechanism used for the direct introduction of the well-defined mesoporosity inside zeolites as shown in Figure 2.8 [70].

The crystal rearrangement is only possible if the base opens the Si-O-Si bonds with the help of cationic surfactant and form the $Si\text{-}O^-$ species. This method prohibits the dissolution of zeolite crystals and allows the useful interaction between surfactant and zeolite. Typically, complete recovery of mesostructured materials achieved after the process. And the material has high hydrothermal stability after the surfactant templated process.

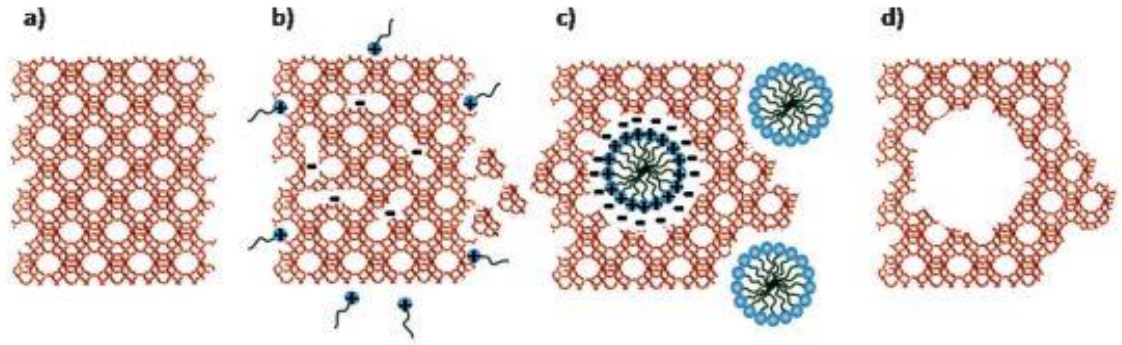

Figure 2.8: Mechanism of surfactant templated mesopores formation [70].

Figure 2.8 described the schematic demonstration of the mechanism of mesopore formation inside zeolite by using the surfactant. In Figure 2.8 (a) represented the original Y-zeolite (b) described the opening of Si-O-Si bond in alkaline media (c) shows the surfactant micelles surrounded by the crystal rearrangement (d) represents the mesopores introduced by removal of surfactant template.

At the start, this technique was only applied to the high silica zeolites (Si/Al = 15) such as USY, mordenite, and ZSM-5. Later on, this method was applied to the high alumina zeolites such as NaY (Si/Al ratio of 1-3) with the addition of acid pretreatment step using inorganic or organic acid [71]. Acid pretreatment steps break some of the Al-O bonds which create some vacancies and wear out the rigidity of the zeolite structure. Subsequent treatment of this treated zeolite with cationic surfactant (CTAB) in the presence of NaOH

or NH_4OH at elevated temperature for 1 hour creates the mesoporous Y-zeolite which has very similar properties to the parent zeolite [70].

2.4.5 Soft templating methods

The method that involves the nonsolid template is called the soft templating method. Soft templates include the surfactants and the block copolymers for creating the mesoporosity. There are certain advantages of using block copolymers i.e. low cost and easy availability [60]. On the other hand, surfactants are also used in direct templating methods. The added surfactants also impart a key role during the re-organization of the zeolite-based FCC catalysts to form the required mesopores. Organosilane surfactants have an important role in the generation of active mesoporosity with less difficulty [72]. Organoline was used as a templating agent for the preparation of hierarchical Y-zeolites assisted by microwave hydrothermal method. The results were shown a better catalytic performance as compared to conventional Y-zeolite [73]. However, phase-disintegration, as well as amorphous phase lining formation problems have been limited the use of surfactant-based methods on an industrial scale. Similarly, there could be a stability problem in the derived catalyst under hydrothermal conditions. Further, polymeric materials are reported as alternative templates [74].

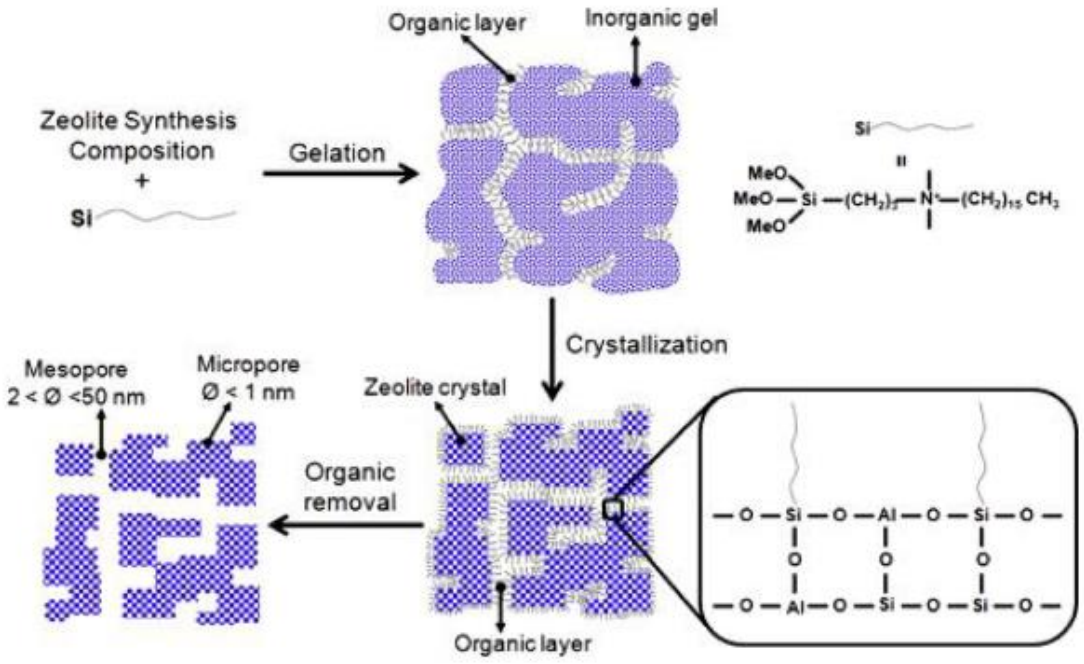

Figure 2.9: Creation of mesopore in zeolites by using organosilane surfactants [64].

2.4.6 Hard templating methods

The method in which we used solid materials is called the hard-templating method. In this method, hierarchical zeolite is synthesized by using carbon materials such as carbon nanofibers, carbon nanotubes as well as ordered mesoporous carbon, etc. [75]. Some other method includes the organosilanes, polymers, resins, biological substrates as well as organic materials i.e., calcium carbonate and magnesium hydroxide. During the process, the excess quantity of zeolite gel affects the zeolite growth around carbon particles. Later, similar results have been achieved by synthesizing the super-ordered mesopores in the range of 3 to 7nm [76]. The hierarchical form of all known zeolites can be achieved by using this approach. Likewise, this method is very useful in the retention of zeolitic and acidic properties. However, some unfavourable factors impeded the use of this method on an industrial scale. High cost, expanded synthesis stages, and selection of suitable porous

carbon materials are these factors [77]. The preparation of hierarchical zeolite with the help of carbonaceous material as a template is presented in Figure 2.10.

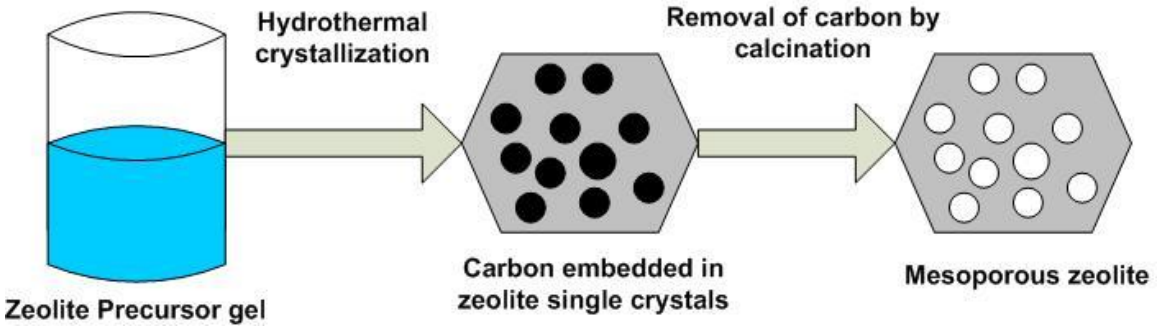

Figure 2.10: Synthesis of hierarchical zeolite using carbonaceous material as a hard template [53].

CHAPTER 3

EXPERIMENTAL METHODOLOGY

This chapter will demonstrate the material used in the experimental studies for the modification in Y-zeolites and FCC catalysts. It also presents the detailed synthesis experimental procedure and techniques used in the characterization of the modified Y-zeolites and FCC catalysts. The evaluation procedure for the testing of FCC catalysts in the MAT unit is also discussed.

3.1 Materials

Following materials were used for the modification of Y-Zeolite and synthesis of FCC catalyst:

- Na-Y zeolite (SiO_2/Al_2O_3 = 5.6) was obtained from CATAL
- Ultra-stable Y zeolite (SiO_2/Al_2O_3 = 6) was obtained from Grace
- Sodium hydroxide was supplied by BDH Analar
- Cetyltrimethylammonium bromide (CTAB), Ammonium nitrate, Kaolin, and Ludox AS-40 was obtained from Sigma Aldrich
- Siral 40 (40% Al_2O_3, 60% SiO_2) was obtained from CONDEA
- Vacuum gas oil (VGO) obtained from a domestic refinery

3.2 Post-treatment of Y-Zeolite

The modification of Y zeolite to obtain the hierarchical zeolite was adopted from the method reported in the literature [33] with some changes in process conditions. The changes in process conditions are mentioned at the end of this experimental procedure.

In a present post-treatment method, a slurry was prepared by mixing 20g of commercial Na-Y Zeolite (SiO_2/Al_2O_3 = 5.6) with 200ml of water. The pH of this slurry was close to 9.0 which was adjusted to 5.5-5.7 by adding a few drops of dilute nitric acid (10% dilute). Afterward, the slurry was stirred with 10% citric acid (using 1.50, 3.65, and 6.0 milliequivalents of acid per 1g of zeolite) for 15min at ambient temperature. Then, acid-treated Y-Zeolite was recovered by vacuum filtration and washed with deionized water. Further, it was re-slurried in distilled water (200ml) containing 0.24M of sodium hydroxide (NaOH) and 10.2g cetyltrimethylammonium bromide (CTAB).

After this solution was poured into a polypropylene bottle and placed in the oven overnight at 100 °C. Next, the treated Zeolite was recovered using vacuum filtration, washed with deionized water, and dried overnight at 110 °C in the oven. A modified zeolite sample was calcined at 550 °C for 5 hours to remove the impurities as well as the organic template. The calcined sample was placed in a desiccator at 100 °C temperature until it is cooled to room temperature. The modified Y-zeolite was three-time ion-exchanged with 0.1M ammonium nitrate solution at 80 °C for 1 hour to obtain the H-form of the zeolite. For each gram of zeolite, 15 ml of 0.1M ammonium nitrate solution was used for ion exchange. Finally, drying overnight and calcination for 1 hour was performed to remove the last traces of moisture. The obtained modified zeolites were denoted as MY30, MY73, and MY120.

Aqeel et al [33] used 5g of CBV-100 (SiO_2/Al_2O_3=5.1), treated with 6 and 9 milli-equivalents of 10% citric acid per 1g of the zeolite for 1hr at ambient temperature. The authors did not mention the molar concentration of NaOH used. The authors used calcination temperature 450 °C for 1hr (flow of nitrogen) and 550 °C for 2hr (oxygen environment). Further, 1mol/L NH_4NO_3 was used for a three-time ion exchange of the sample without mentioning liquid to solid ratio.

3.3 Preparation of FCC catalyst using USY zeolite

A series of FCC catalysts were synthesized with five different compositions (weight %) of Ultra-stable Y-zeolite (USY) and matrix as given in Table 3.1. The amount of USY used in this preparation was in the range of 15 wt. % to 34 wt. %. These percentages were selected to fall in the range (15-45 wt.%) as described in the literature [78]. The USY of less than 15% decreases the activity of the catalyst and more than 45% increases the attrition rate.

Siral 40, Ludox AS-40, and kaolin were used for amorphous silica-alumina, silica solution, and clay respectively in the approximate ratio of 1:2:5 to make a consistent matrix. All four components, namely: USY, Siral 40, Ludox AS-40, and kaolin were mixed in de-ionized water for the preparation of FCC catalyst. Afterward, the slurry was heated above 100 °C with continuous magnetic stirring until it became dry. The mixture was then placed in the oven at 110 °C for overnight drying. The dried product was crushed and calcined at 550 °C for 6 hours. Finally, 12 g of each prepared sample was treated with 100% steamed at 750 °C for 5 hours. The steamed catalyst was sieved for the proper particle size (500-850 µm) before micro activity testing. After steaming, USY based FCC catalyst names were used St-Y01, St-Y02, St-Y03, St-Y04, and St-Y05.

Table 3.1. Chemical composition of USY based FCC catalysts.

Name of catalyst	USY (wt. %)	Siral 40 (wt. %)	Ludox AS-40 (wt. %)	Kaolin (wt. %)	Zeolite/Matrix Ratio
St-Y01	15	11	21	53	18
St-Y02	20	10	20	50	25
St-Y03	23	10	19	48	30
St-Y04	26	9	19	46	35
St-Y05	34	8	17	42	50

3.4 Preparation of FCC catalyst using modified Y-zeolite

Three FCC catalysts (St-Y30, St-Y73, and St-Y120) were prepared by using three modified zeolites (MY30, MY73, and MY120) and a matrix. The matrix of FCC catalyst consisted of amorphous silica-alumina, silica solution, and clay which were chemically obtained from Siral 40, Ludox AS-40, and kaolin respectively. All four components modified Y-zeolite, Ludox AS-40, Siral 40, and kaolin were mixed in water with the percentages mentioned in Table 3.2, to make 18% Zeolite/Matrix FCC catalyst slurry. Thereafter, slurry was heated above 100 °C with continuous magnetic stirring until it became dry. The slurry was then placed in the oven at 110 °C for overnight drying. Afterward, the dried product was crushed and calcined at 550 °C for 6 hours. Finally, 12 g of prepared sample was 100% steamed at 750 °C for 5hr. The steamed catalyst was sieved for the proper particle size (500-850 µm) before micro activity testing. After steaming, the modified FCC catalyst names were used St-MY30, St-MY73, and St-MY120.

Table 3.2. Chemical composition of modified zeolite-based FCC catalysts.

Name of catalyst	Modified Zeolite (wt. %)	Siral 40 (wt. %)	Ludox AS-40 (wt. %)	Kaolin (wt. %)	Zeolite/Matrix Ratio
St-MY30	15	11	21	53	18
St-MY73	15	11	21	53	18
St-MY120	15	11	21	53	18

3.5 Characterization of catalyst

All FCC catalysts and Zeolite samples were characterized for their physical and chemical properties by using the following techniques.

3.5.1 X-ray diffraction

The crystallinity of as-synthesized FCC catalyst samples was determined by X-ray powder diffraction technique using a Rigaku Miniflex II with nickel filtered CuKα radiation having a wavelength of λ = 1.5406Å at 30mA and 40kV operating parameters. Diffraction pattern was generated for 2 theta from 3° to 50° with a scan rate of 3°/min.

3.5.2 BET surface area and pore size distribution

Textural properties of the samples were measured by using Micromeritics ASAP-2020 sorption analyzer with the help of nitrogen adsorption at -196 °C. A 100 mg of calcined sample was taken for BET surface area measurement. Before nitrogen physisorption, the samples were degassed under vacuum (10^{-5} torr) at 350 °C for 3 hours. Adsorption isotherms of the samples were measured at -196 °C (liquid nitrogen temperature). Pore size distribution and surface areas were calculated by using the Barrett Joyner Halenda (BJH) and Brunauer Emmet-Teller (BET) methods, respectively.

3.5.3 Inductively Coupled Plasma Analysis

Silica to alumina (SiO_2/Al_2O_3) ratio in different FCC samples was measured by using ICP optical emission spectrometer (ULTIMA 2, Horiba Scientific).

3.5.4 Scanning electron microscopy

Scanning electron microscopy (SEM) on TESCAN instrument developed by Oxford coupled with EDX analyzer was used to analyze the morphology as well as the size of the crystals.

3.5.5 Temperature programmed desorption

Ammonia temperature-programmed desorption (TPD) was used for acidity measurements in the BELCAT equipment. Calcined sample (100mg) was pre-treated at 500 °C for 1 hour in the presence of Helium (He) with a 50ml/min flow rate. Afterward, the sample was cooled down to 100 °C and exposed to NH_3/He mixture with a volume ratio (%) of 5/95 at 100 °C for 30 minutes. Ammonia gas was removed using He purges for 1 hour and then temperature was raised to 600 °C at the rate of 10 °C/min with the same flow of He to perform TPD measurement. TCD detector was used to monitor the desorbed NH_3 gas.

3.6 Evaluation of catalyst

All FCC catalysts were evaluated in the MAT unit based on the product yields of gasoline, LCO, HCO, and coke at 550 °C using VGO as feed.

3.6.1 Micro activity test procedure

Micro activity test (MAT) unit (Sakuragi Rikagaku, Japan) is a fixed bed reactor that was used to investigate the cracking of VGO as shown in Figure 3.1. The properties of Hydrotreated VGO are listed in Table 3.3. ASTM D-3907 method was followed for the

FCC catalyst activity measurement by MAT unit. The time on stream was 30 seconds and the system temperature was set at 550 °C. The amount of the catalyst used for the experiment was 3.0 g and the amount of the vacuum gas oil was 1.0 g. After completion of the reaction, stripping of the products was done in the presence of 30 cc/min of nitrogen for 9 minutes. Considering the high volatility of the liquid products, a circulating bath at -10 °C low temperature was added to the MAT unit instead of the conventional iced water.

During the cracking reaction as well as stripping modes, a burette was used for gas collection from the outlet of the liquid receiver. For obtaining the exact weight of the vacuum gas oil feed, the weight of the syringe before and after the reaction was measured. The MAT operating conditions are summarized in Table 3.4.

Table 3.3. Properties of MAT Feed Oil.

Property	Value
Density (15 °C) (g/cm^3)	0.88
Nitrogen (ppm)	172
Sulfur (ppm)	298
Aromatics (wt. %)	42
Saturates (wt. %)	60
Residue (wt. %)	0.9
Distillation data (vol %)	Temperature (°C)
Initial boiling point	310
5%	345
25%	375
50%	422
90%	510
Final boiling point	565

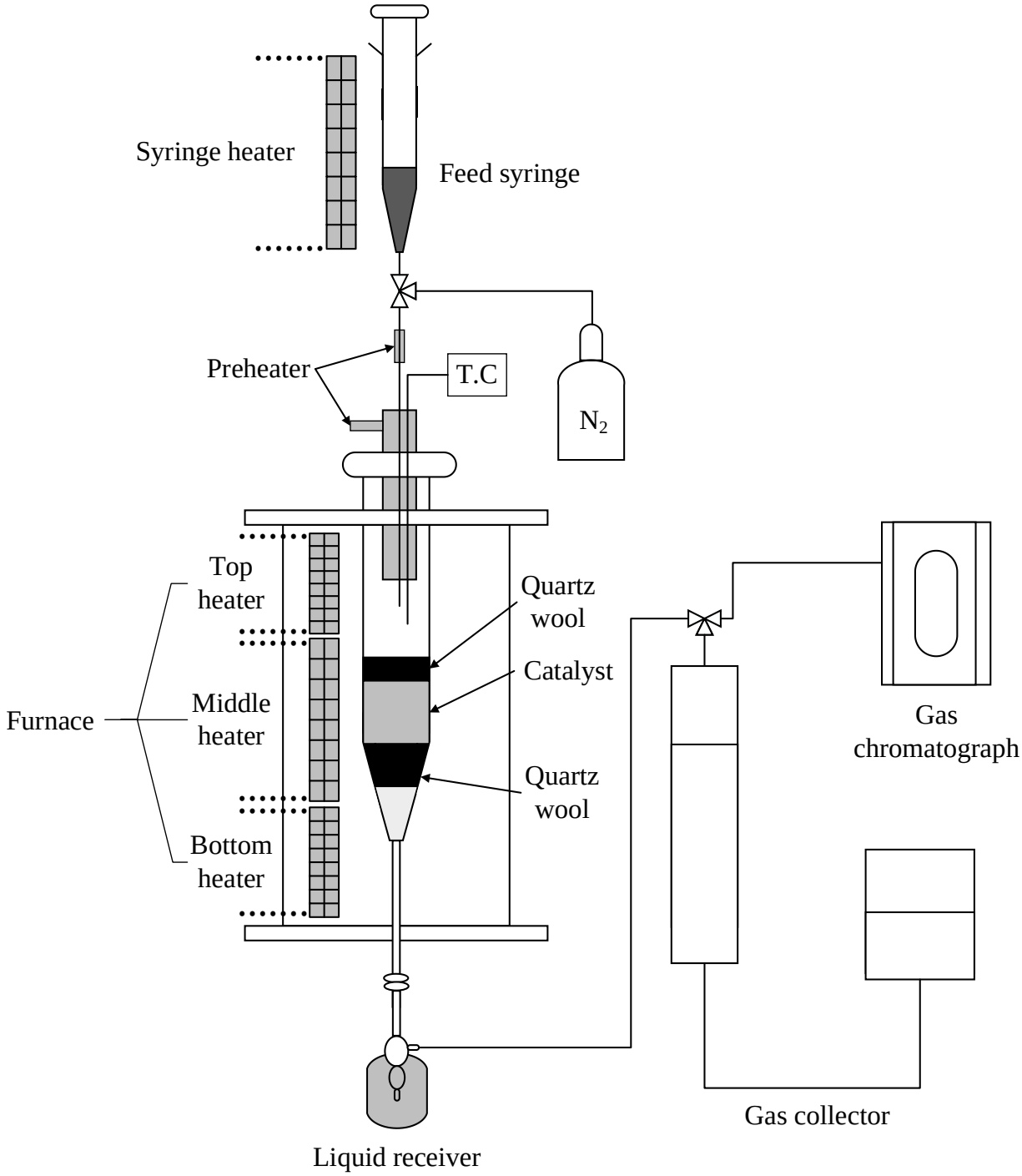

Figure 3.1: Micro activity test (MAT) unit.

Table 3.4. MAT operating conditions.

Property	Value
Feed weight injected	About 1.0 g
Catalyst weight	3.0 g
Feed injection time (Time on stream)	30 s
Feed syringe temperature	Room temperature
Feed injector temperature	5 °C higher than the reaction temperature
Liquid receiver temperature	-9 °C
Catalyst/liquid stripping time	Total 9 min
with a receiver in a cold bath	5 min
with cold bath removed	4 min

3.6.2 Analysis of MAT products

Reaction products of MAT unit contain liquid phase, gaseous phase, and coke on the spent catalyst after the reaction. An acceptable mass balance limit was 95-103% of the injected liquid vacuum gas oil feed. All MAT products were analyzed by gas chromatography to estimate the yield pattern as well as information of the feed being tested on the catalyst. Gaseous products were analyzed using a Micro GC Agilent 3000A equipped with four Thermal Conductivity Detectors (TCD). This Micro GC determined all light hydrocarbons including C_4, C_5 paraffin, H_2 as well as fixed gases. All hydrocarbons from C_1 to C_4 as well as C_5 paraffin were accurately determined. The weight of all light hydrocarbons up to C_4 was added together, and heavier than C_4 hydrocarbons were added to the weight of the liquid product after the analysis. Horiba Carbon-Sulfur analyzer Model EMIA-220V was used to analyze coke deposited on the catalyst. One gram of the spent catalyst was burnt in a furnace at high temperature using tin and tungsten as combustion promoters. Carbon content as a percentage of catalyst weight was calculated with the help of resulting

combustion gas (CO_2) passed through the Infra-Red analyzer. Liquid products were analyzed by Shimadzu GC 2010 equipped simulated distillation according to ASTM method D-2887. Liquid products usually consist of gasoline, LCO, and HCO. The conversion of vacuum gas oil is reported as a sum of gasoline, total gases including (dry gas & LPG) and coke. HCO and LCO with boiling points above 221°C were considered as unconverted feedstock.

CHAPTER 4

RESULTS AND DISCUSSIONS

This chapter will describe the characterization results of all modified Y-zeolites, modified Y-zeolite base FCC catalysts as well as USY base FCC catalysts. Additionally, it will discuss the effect of zeolite to matrix ratio on VGO cracking in MAT unit and comparison of modified Y-zeolite base FCC catalyst with USY base FCC catalyst for zeolite to matrix ratio of 18.

4.1 Characterization of modified Y-zeolites

Three modified Y-zeolites (MY30, MY73, and MY120) and parent zeolite (Na-Y zeolite) are characterized using X-ray diffraction, BET, inductively coupled plasma (ICP), NH3-TPD, and scanning electron microscopy.

4.1.1 X-ray Diffraction

XRD analysis was carried out in this study to monitor the structural changes that occurred in modified zeolites with different acid concentrations. Figure 4.1 demonstrates the XRD measurements of mesoporous Y-zeolites synthesized by treatment with acid and base in the presence of a surfactant used as a template. From Figure 4.1, it can also be noted that the intensity of XRD patterns decreased for treated zeolites (MY30, MY73, and MY120) as compared to the parent zeolite (Na-Y zeolite) with the increase in severity of the acid treatment conditions. The decrease in intensity of XRD patterns is directly related to the apparent decrease in crystallinity which occurs due to the structural degradation of the modified zeolites and intractrystalline mesoporosity created as a result of such treatment.

The structural degradation as a result of acid treatment can be explained by the cleavage of Al-O bond [70]. XRD measurements also reveal that mesoporous zeolites sustain significant crystallinity under relatively mild conditions used for their post-treatment methods. However, the crystallinity of the treated zeolites could be decreased significantly with the severe condition used for the acid or base treatment. The generation of mesoporosity inside the zeolite structure has been achieved without a significant loss of crystallinity in accord with the previous literature [79, 80]. Figure 4.2 shows the low angle XRD analysis with only one peak found at 1.6º for the modified sample (MY120) which indicates the significant degree of the long-range mesopore. On the other hand, MY30 and MY73 have been detected with no peaks at a low angle which shows no significant long-range mesoporous ordering after the treatment.

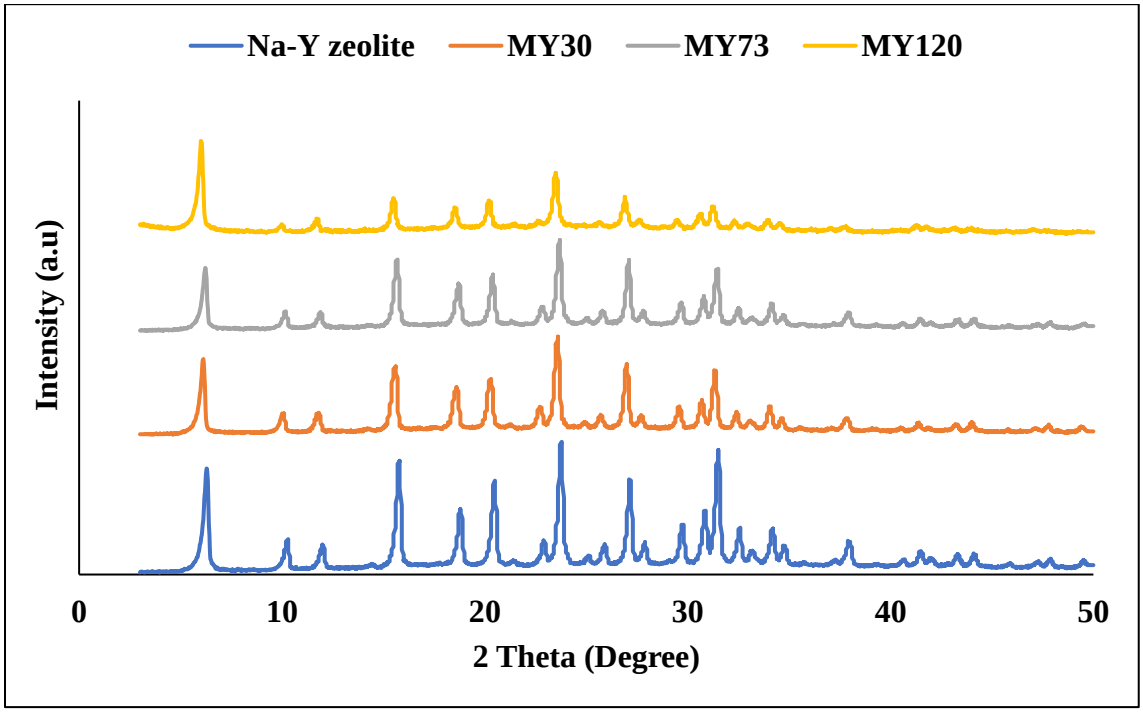

Figure 4.1: XRD patterns of Parent (Na-Y zeolite) and modified Y-zeolite (MY30, MY73, and MY120).

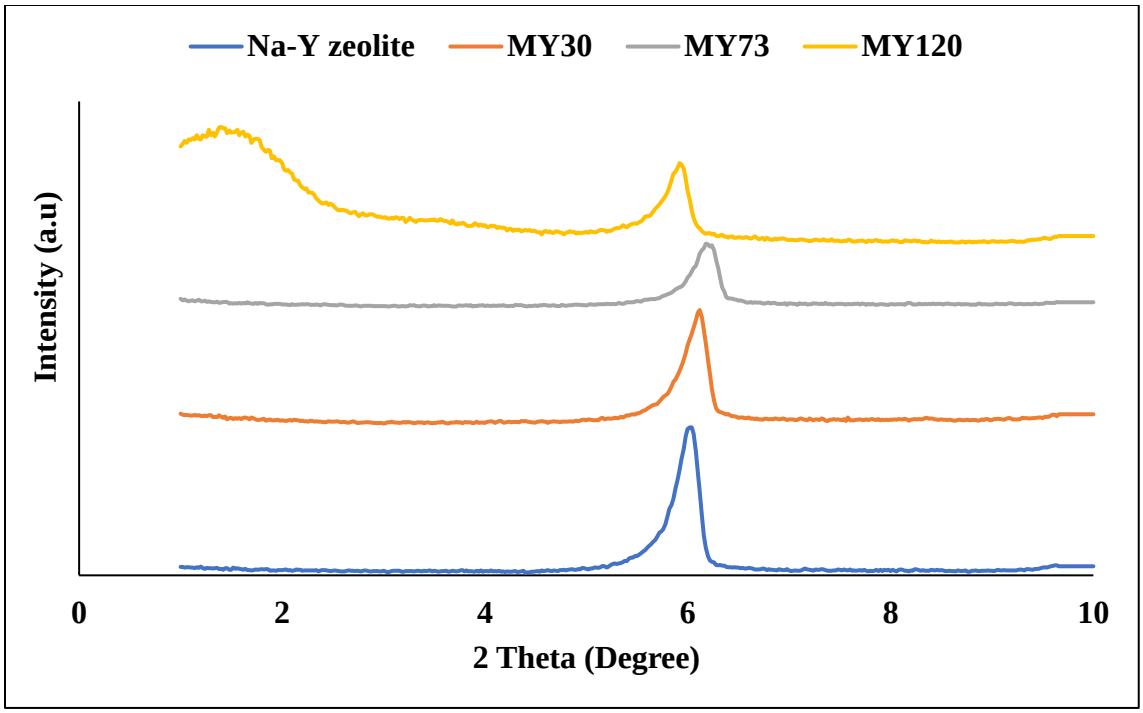

Figure 4.2: Low angle XRD patterns of the parent (Na-Y zeolite) and modified Y-zeolite (MY30, MY73, and MY120).

4.1.2 Surface area and pore structure

Table 4.1 shows the chemical and physical properties of the parent and modified Y-zeolites in the presence of acid, base, and surfactant. N_2 adsorption-desorption analysis showed that treated MY30, MY73, and MY120 samples have a surface area of 615 m^2/g, 634 m^2/g, and 650 m^2/g as compared to 683 m^2/g of parent Na-Y zeolite. Further, it is indicated that micropore volume is decreased and mesopore volume is increased for MY30, MY73, and MY120 samples. For example, micropore volume of both MY30 and MY-73 decreased by 15%, while a 36% decrease was noted for MY120 as compared to parent Y-zeolite micropore volume. On the other hand, mesopore volume of 0.08 cc/g, 0.16 cc/g, and 0.30 cc/g was observed for MY30, MY73, and MY120 respectively as compared to 0.03 cc/g for the starting Na-Y zeolite mesoporous volume. Total pore volume of MY30 remains same as compared to parent Y-zeolite, whereas significant increase in total pore volume

has been observed for MY73 and MY120. Figure 4.3 (a), (b), and (c) show the N_2 adsorption-desorption data of the isotherm's profiles for the MY30, MY73, and MY120 samples as compared with parent zeolite. It shows the type I isotherm for the parent zeolite and MY30 and type IV for the MY73, and MY-120 samples. For treated Y-zeolites, H4 type hysteresis loop is noticed (less evident for MY30), which is related to mesoporous zeolites having a bimodal pore size distribution that highlighted the presence of both micro and mesopore [81]. From Figure 4.3, it is seen that MY120 and MY73 exhibits a remarkable N_2 uptake at relative pressure (p/p_o) greater than 0.4 showing the presence of a larger mesopore as compared with MY30, which indicated a sharp Barrett Joyner Halenda (BJH) pore size distribution [82] around 4 nm (size of a CTAB micelles) [70].

Table 4.1. Chemical and physical properties of parent (Na-Y zeolite) and modified Y-zeolites.

Zeolite	Surface area	Micropore volume	Mesopore volume	Total pore volume	SiO_2/Al_2O_3 ratio[b]	Total acidity
	(m^2/g)[a]	V_{mic} (cc/g)	V_{mes} (cc/g)	(cc/g)	-	(mmol/g)[c]
Na-Y zeolite	683	0.33	0.03	0.36	5.6	-
MY30	615	0.28	0.08	0.36	7.1	0.724
MY73	634	0.28	0.16	0.43	7.8	0.700
MY120	650	0.21	0.30	0.51	9.3	0.578

[a] Measured by BET method [b] Determined by ICP analysis [c] Measured by Ammonia TPD

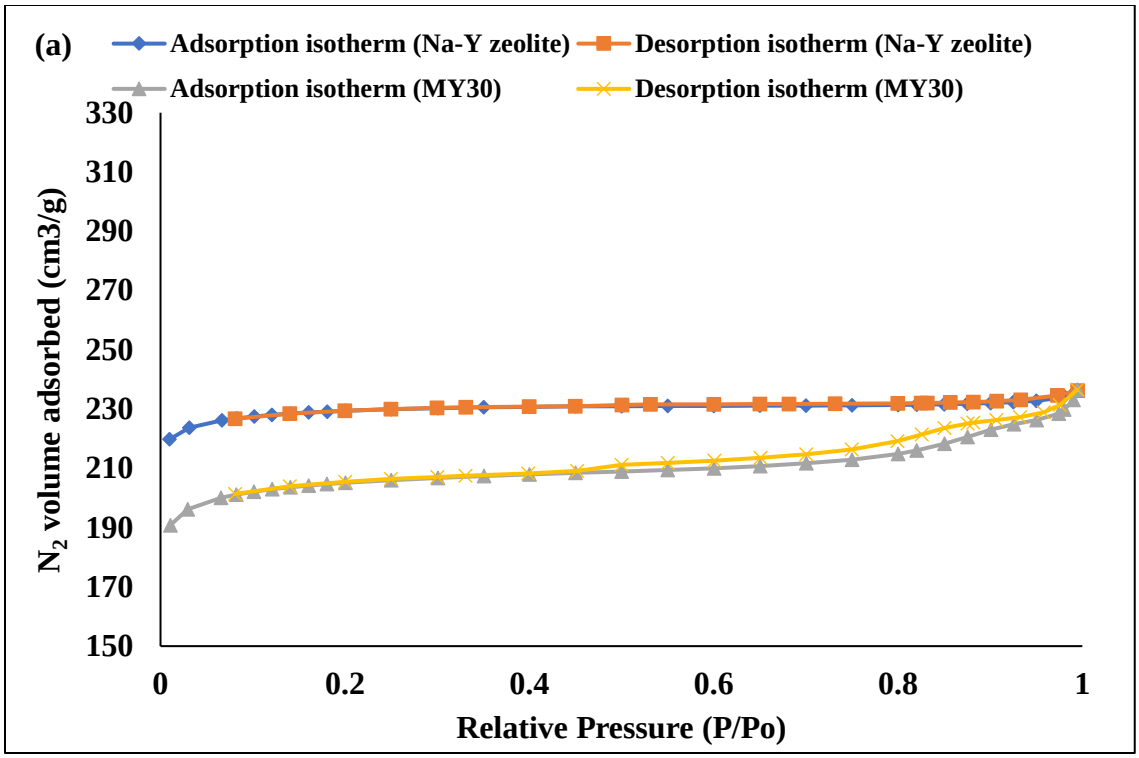
(a)
Adsorption isotherm (Na-Y zeolite)
Desorption isotherm (Na-Y zeolite)
Adsorption isotherm (MY30)
Desorption isotherm (MY30)
330
310
290
270
250
230
210
190
170
150
N2 volume adsorbed (cm3/g)
0
0.2
0.4
0.6
0.8
1
Relative Pressure (P/Po)

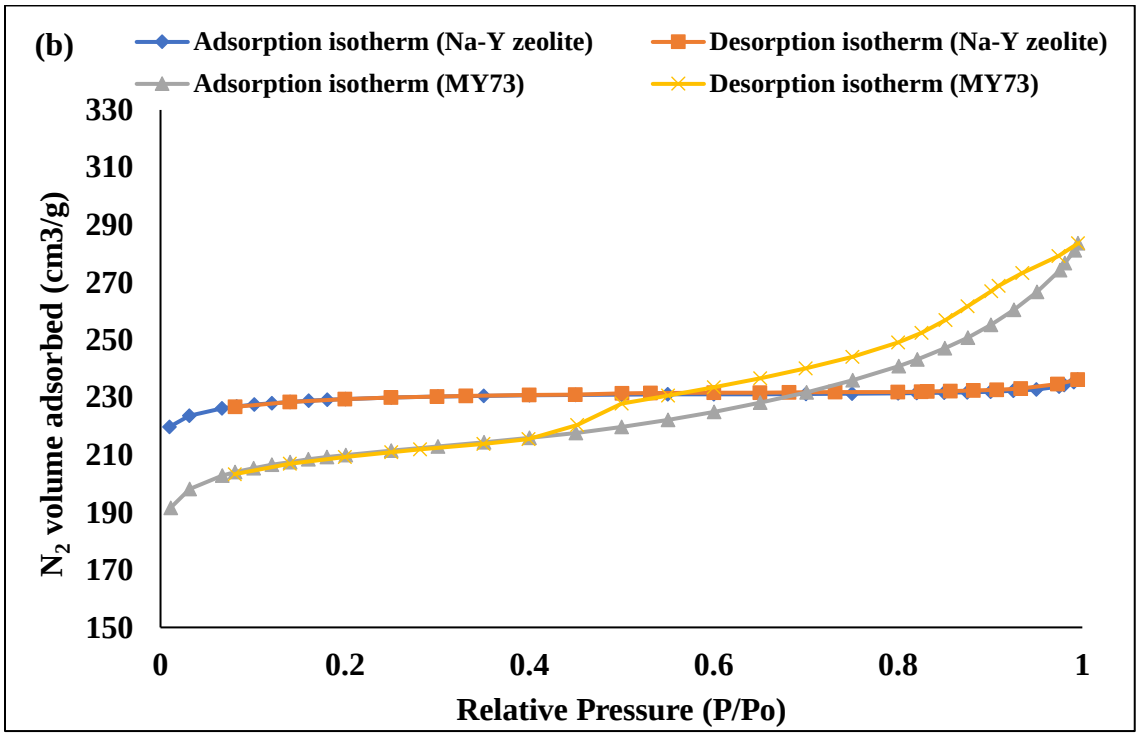
(b)
Adsorption isotherm (Na-Y zeolite)
Desorption isotherm (Na-Y zeolite)
Adsorption isotherm (MY73)
Desorption isotherm (MY73)
330
310
290
270
250
230
210
190
170
150
N2 volume adsorbed (cm3/g)
0
0.2
0.4
0.6
0.8
1
Relative Pressure (P/Po)

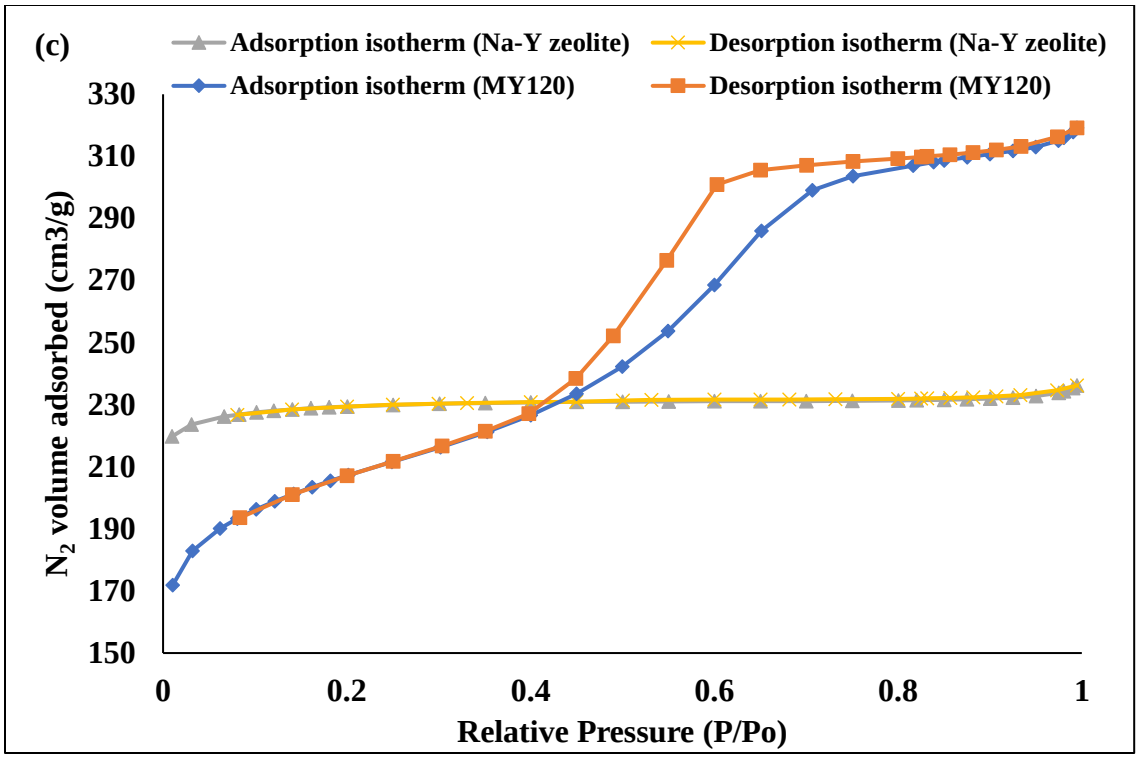

Figure 4.3: N_2 adsorption-desorption isotherms of the parent and modified Y-zeolites: (a) MY30 (b) MY73 (c) MY120.

Figure 4.4 shows the pore size distribution of parent and modified Y-zeolite samples. It is seen that differential pore volume substantially increased for the MY120 sample after treatment as compared to the parent Y-zeolite sample, whereas the MY30 sample has not shown a significant increase at low citric acid concentration. The differential pore volume of MY73 lies in between MY30 and MY120. It is indicated that MY120 has the highest pore volume after modification among MY30 and MY73.

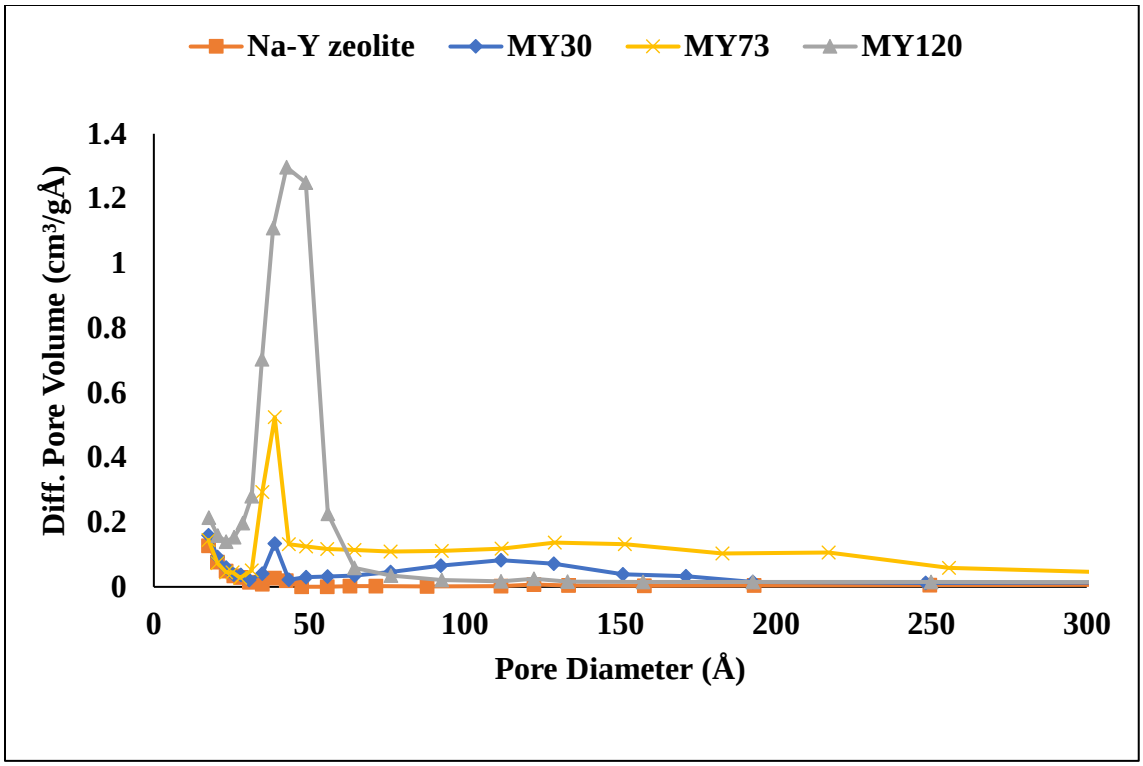

Figure 4.4: Pore size distribution of parent and modified Y-zeolites.

The textural properties of treated zeolites depend on the acid or base concentration, contact times as well as surfactant type used in post-treatment. From Table 4.1, it is noted that mesopore volume increases with an increase in acid concentration for MY30, MY73, and MY120 samples, while a large part of micropore volume is conserved which is in good agreement with the literature [33]. Mesoporous zeolites modified in the presence of surfactant (CTAB) have more pore volume and crystallinity due to the generation of controlled intracrystalline mesoporosity. On the other hand, the materials modified using NaOH/KOH in the absence of surfactants have low pore volume and crystallinity [83]. The discovery of surfactant templated mesoporous zeolite was made in 2004 [84]. However, this method was only applied for high silica zeolite materials such as CBV720 (Si/Al = 15). Recent developments have been made to apply this method for high alumina materials

such as USY, Na-Y, and NH_4-Y (Si/Al = 2.5-3), which are used in catalytic cracking of heavy oils [30]. During the treatment of medium and high silica zeolites (Si/Al = 8-20), the combination of basic media and surfactant is used to protect the structure of zeolite from excessive desilication where some of the Si-O-Si bonds are broken to create negatively charged sites in zeolite structure. These negatively charged sites are balanced by the cationic surfactant. On the other hand, Si-O-Al bond is difficult to break for low silica zeolites in basic media. Hence, using an extra acid pre-treatment step is important before introducing the combination of base and surfactant. Therefore, a dilute citric acid was used to start the dealumination process by breaking the O-Al bonds which slightly increase the bulk Si/Al ratio. The acid pre-treatment step generates a sufficient amount of defects in zeolite structure which facilitated the creation of mesoporosity through subsequent surfactant templating step. The negatively charged zeolite sites of $Si\text{-}O^-$ and cationic surfactant are attached together by electrostatic attraction. The molecules of the surfactant self-assemble to form micelles inside the zeolite structure to create the intractrystalline mesoporosity [81].

4.1.3 Inductively coupled plasma (ICP) analysis

From Table 4.1, we can see the increase in the SiO_2/Al_2O_3 mole ratio for modified zeolite samples with an increase in the severity of acid concentration at a constant molar concentration of NaOH and CTAB. Parent zeolite (Na-Y zeolite) has a SiO_2/Al_2O_3 ratio of 5.6. The ratio was increased to 7.1 for MY30 due to dealumination and desilication both in the presence of citric acid treatment. Similarly, the SiO_2/Al_2O_3 ratio of 7.8 and 9.3 was noted for MY73 and MY120, respectively.

4.1.4 Temperature Programmed Desorption (NH_3-TPD)

This method was used to determine the total acidity of the modified zeolite samples. Figure 4.5 shows the temperature desorption peaks of MY30, MY73, and MY120 at temperatures between 100-600 ºC. From Table 4.1, it is indicated that MY30 and MY73 have total acidity of 0.724 mmol/g and 0.700 mmol/g, whereas 0.578 mmol/g acidity was for MY120. It is noted that the acidity of the modified zeolite samples decreases as the dealumination increases from sample MY30 to MY120.

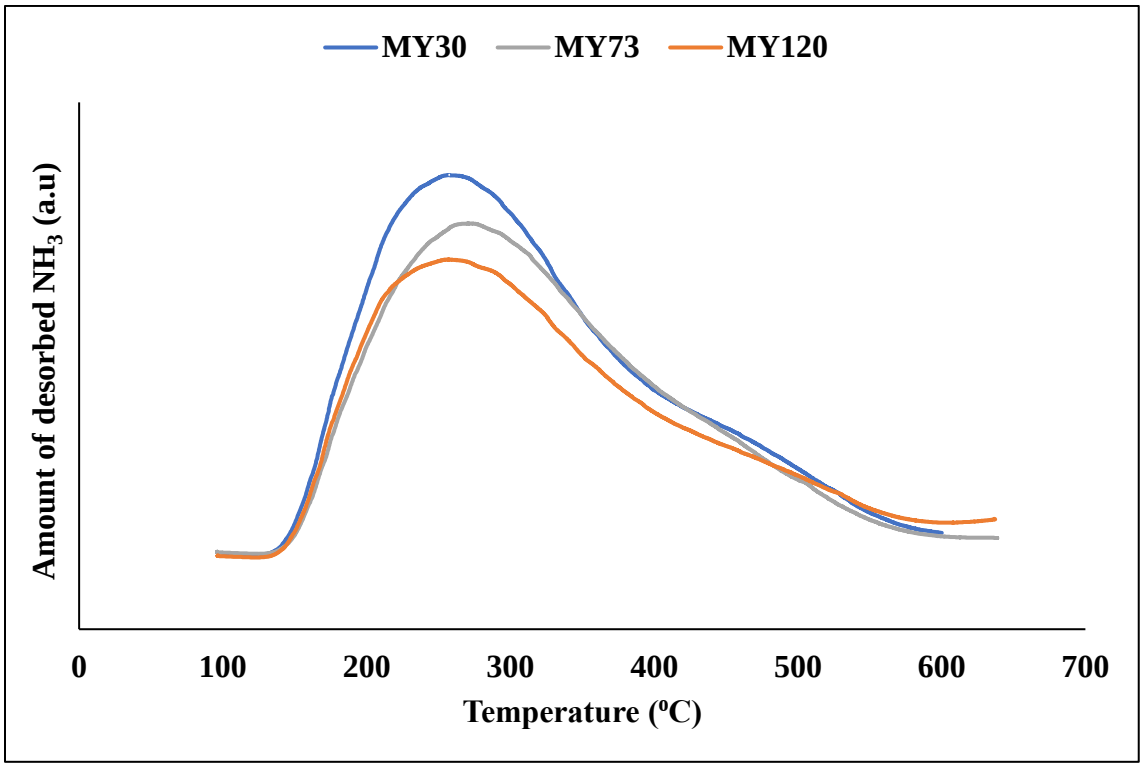

Figure 4.5: NH_3 temperature-programmed desorption of the modified zeolites.

4.1.5 Scanning Electron Microscopy

Figure 4.6 shows the surface morphology of modified zeolites (MY30, MY73, and MY120) at a scale bar of 0.5μm and 27k magnifications. The SEM images of modified zeolite samples showed similar morphology as compared with the parent (Na-Y zeolite) reported in the literature [70]. Moreover, no major clusters were observed on the surface of the zeolites after the post-treatment.

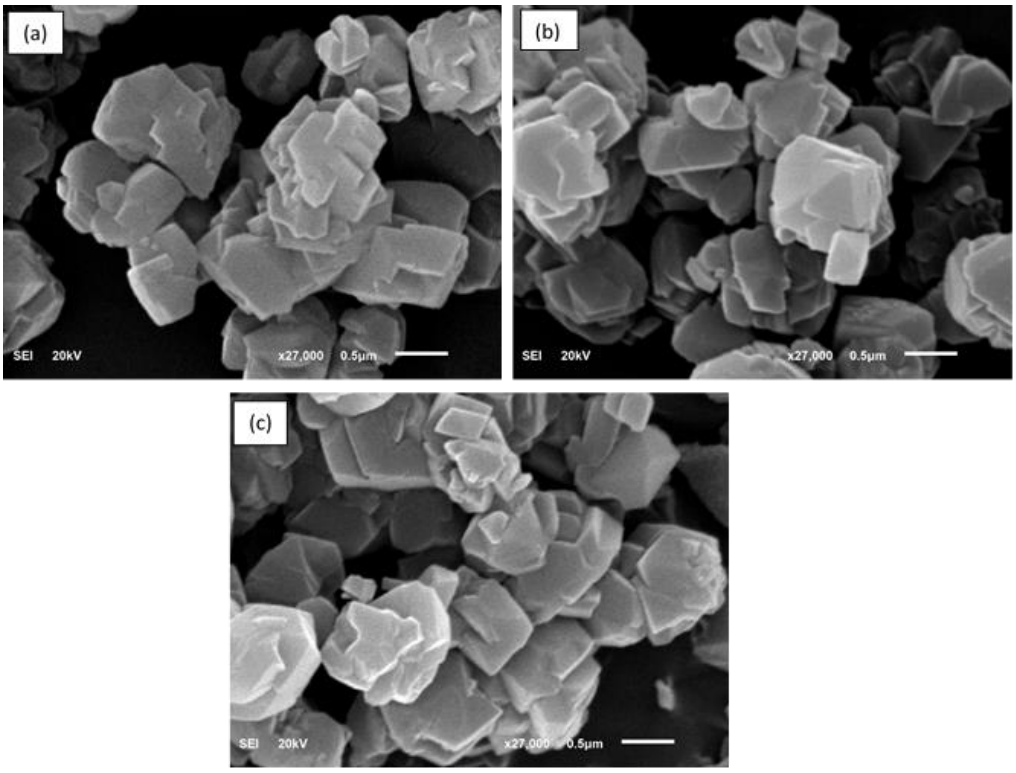

Figure 4.6: SEM images of Modified Zeolites (a) MY30 (b) MY73 (c) MY120.

4.2 Characterization of modified Y-zeolites based FCC catalysts

The comparison of XRD patterns of modified Y-zeolite based steamed FCC catalyst samples are shown in Figure 4.7. The XRD patterns of all FCC catalysts demonstrate that only the Y-zeolite structure corresponds to the XRD pattern of Y-zeolite reported in the literature [85] and no other zeolite characterizing peaks were observed in the pattern. The

intensity of XRD peaks in all samples after steaming was decreased due to a loss of its surface area. The steaming conditions were set so that the steamed catalyst has properties similar to the equilibrium catalysts (E-Cat) used in commercial FCC units.

Table 4.2 demonstrates the chemical and physical properties of steamed FCC catalysts i.e. surface area, micro and mesopore volume, SiO_2/Al_2O_3 ratio, and acidity of the catalysts. The surface area of St-MY120 reached 112 m^2/g while for MY120 the surface area was 125 m^2/g. Similar to the surface area, the acidity of the modified samples decreased due to an increase in the dealumination process from St-MY30 to St-MY120. It was 0.027, 0.027, and 0.020 mmol/g for St-MY30, St-MY120, and St-MY120, respectively. Figure 4.8 shows the temperature desorption peaks of St-MY30, St-MY73, and St-MY120 at temperatures between 100-600 ºC. From Table 4.2, it has been observed that the micropore volume of the FCC catalyst decreased and mesopore volume increased. Further, total pore volume was increased from St-MY30 to St-MY120.

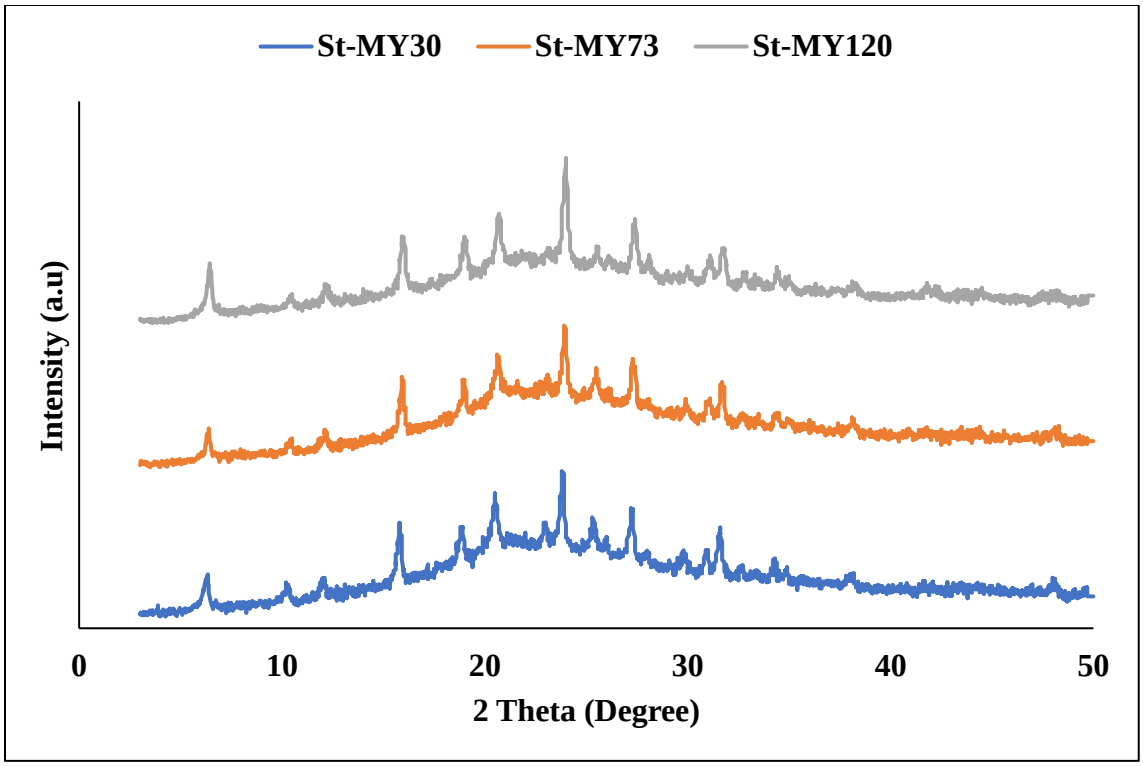

Figure 4.7: XRD pattern of modified Y-zeolite based FCC catalysts.

It can be observed that micropore volume decreased by 26% and mesopore volume increased by 17% for St-MY120 as compared to St-MY30. On the other hand, the total pore volume was increased by 12% for St-MY120. It is noted that the micropore volume of St-MY30 and St-MY73 has not changed significantly due to which the acidity of these two samples remains the same. It is also indicated that silica to alumina ratio increases from St-MY30 (SiO_2/Al_2O_3=6.2) to St-MY120 (SiO_2/Al_2O_3 = 7.2).

Table 4.2. Chemical and physical properties of as-synthesized modified Y-zeolite based FCC catalysts.

Zeolite	Surface area	Micropore volume	Mesopore volume	Total pore volume	SiO_2/Al_2O_3 ratio[b]	Total acidity
	(m^2/g)[a]	V_{mic} (cc/g)	V_{mes} (cc/g)	(cc/g)	-	(mmol/g)[c]
St-MY30	124	0.034	0.224	0.25	6.2	0.027
St-MY73	117	0.032	0.242	0.27	6.6	0.027
St-MY120	112	0.025	0.264	0.28	7.2	0.020

[a] Measured by BET method [b] Determined by ICP analysis [c] Measured by Ammonia TPD

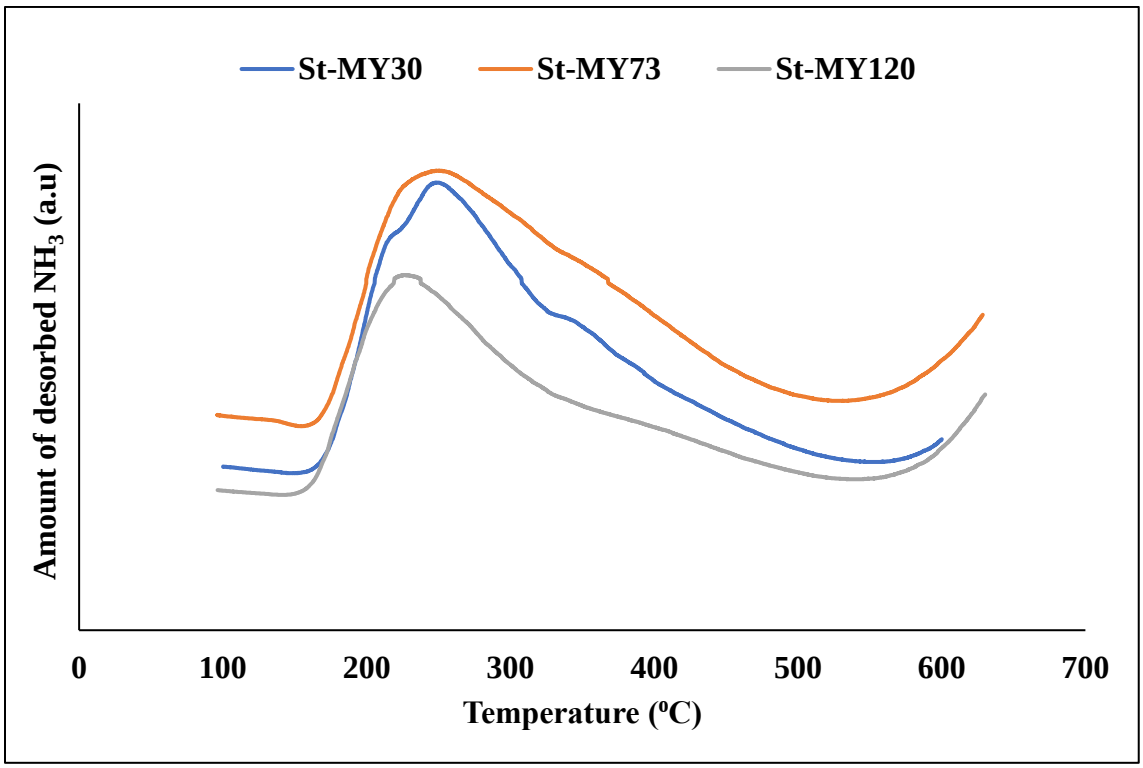

Figure 4.8: NH_3 temperature-programmed desorption of the modified zeolite-based FCC catalysts.

4.3 Characterization of USY based FCC catalysts

Five USY based FCC catalysts (St-Y01, St-Y02, St-Y03, St-Y04, St-Y05) was prepared with a zeolite to matrix ratio of 18 to 50. These samples were prepared to study the effect of zeolite to matrix ratio on product yields of gasoline, LCO, HCO, and coke after VGO cracking at 550ºC. The comparison of XRD patterns of steamed FCC catalyst samples is shown in Figure 4.9. The similarity in XRD patterns after steaming indicated that the steaming at higher temperatures did not substantially, change the crystalline structure of the FCC catalysts.

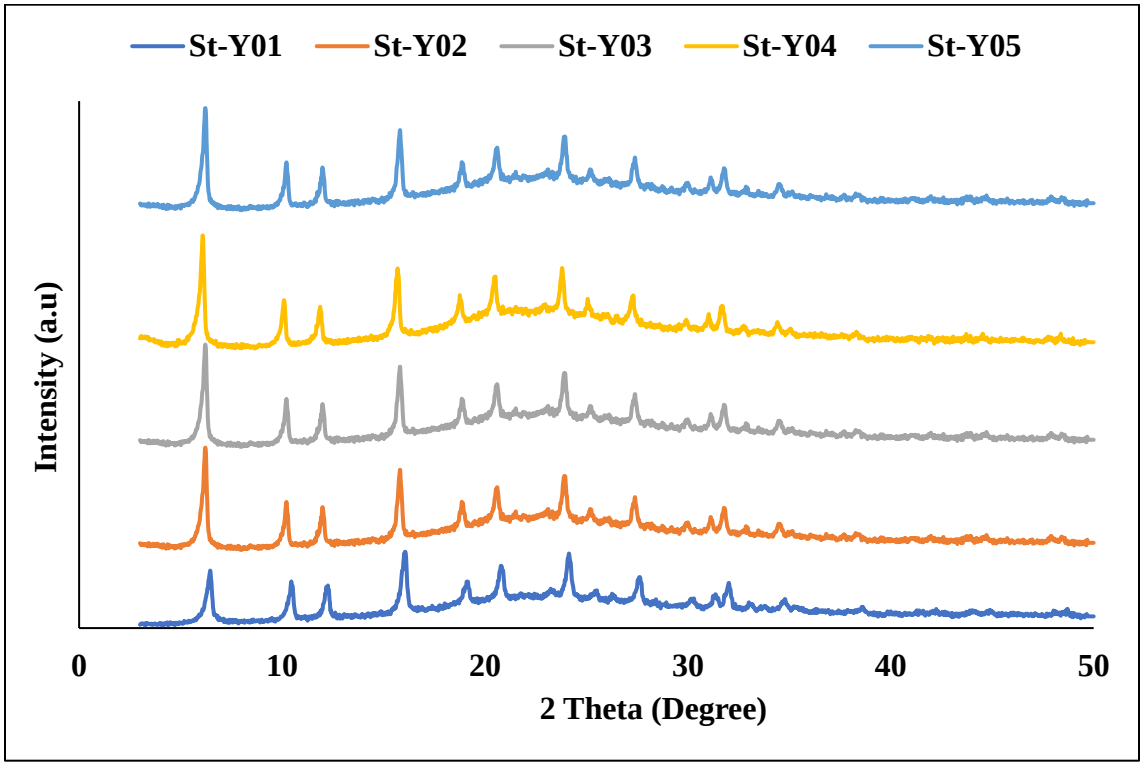

Figure 4.9: XRD patterns of USY based FCC catalysts.

The effect of zeolite to matrix ratio on the surface area, total pore volume, SiO_2/Al_2O_3 ratio, and acidity of the catalysts are listed in Table 4.3. It is shown that the surface area increases directly with the increase of zeolite to matrix ratio when the range goes from 18

to 50. The surface area for St-Y01 was 124 m^2/g while for St-Y05 it was 202 m^2/g. Table 4.3 also shows the effect of zeolite to matrix ratio on the acidity, micro, and mesoporous volume of the FCC catalysts. Like the surface area, the acidity of the FCC catalysts increased with the increase in zeolite to matrix ratio. For St-Y01, the acidity was 0.072 mmol/g. As expected, the acidity increased by an increase in zeolite to matrix ratio; for instance, it reached 0.09, 0.10, and 0.11 mmol/g for St-Y02, St-Y03, and St-Y04 samples. For zeolite to matrix ratio of 50, the acidity of the sample increased by 94% as compared to St-Y01 sample acidity. The acidity of the FCC catalyst is directly related to the activity of the catalyst. Hence, the steaming of the FCC catalyst simulates the deactivation to form the equilibrium catalyst similar to the commercially used catalyst.

Table 4.3: Chemical and physical properties of as-synthesized USY based FCC catalysts.

Catalyst	Surface area	Micropore volume	Mesopore volume	Total pore volume	SiO_2/Al_2O_3 ratio[b]	Total acidity
	(m^2/g)[a]	V_{mic} (cc/g)	V_{mes} (cc/g)	(cc/g)	-	(mmol/g)[c]
St-Y01	125	0.039	0.220	0.25	3.42	0.072
St-Y02	146	0.048	0.212	0.25	3.55	0.090
St-Y03	160	0.055	0.207	0.25	3.65	0.10
St-Y04	173	0.064	0.202	0.26	3.72	0.11
St-Y05	202	0.080	0.190	0.27	3.94	0.14

[a] Measured by BET method [b] Determined by ICP analysis [c] Measured by Ammonia TPD

Table 4.3, it has been observed that the micropore volume of the FCC catalyst increased and mesopore volume decreased with the increase in zeolite to matrix ratio from 18 to 50. It can be observed that micropore volume increased by 105% and mesopore volume decreased by 13% for St-Y05 (Zeolite/Matrix=50) as compared to St-Y01 (Zeolite/Matrix=18). The total pore volume of St-Y01, St-Y02, and St-Y03 remains the same 0.25 cc/g, while 0.26 and 0.27 cc/g was calculated for St-Y04 and St-Y05,

respectively. It is also indicated that the overall silica to alumina ratio is slightly increased from 3.42 to 3.94 for an increase in zeolite to matrix ratio from 18 to 50.

4.4 Evaluation of USY based FCC catalysts

The distribution of product yields because of VGO cracking over five steamed FCC catalysts are reported in Table 4.4. The conversion of VGO is defined as 100 – (Light cycle oil (LCO) wt. % + Heavy cycle oil (HCO) wt. %) since VGO contains light and heavy cycle oil both.

From Table 4.4, it is indicated that vacuum gas oil conversion increased from 76% to 81% (550°C and C/O = 3) by increasing zeolite to matrix ratio of 18 (St-Y01) to 50 (St-Y05). This increment in vacuum gas oil conversion with an increase in zeolite to matrix ratio is due to a rise in surface area and acidity both, in steamed FCC catalysts. Figure 4.10 shows the trend of increasing conversion (%) of steamed FCC catalyst samples. Overall, a 5.8% increase in conversion was calculated for the steamed FCC samples (from St-Y01 to St-Y05).

Table 4.4. Different (%) Zeolite/Matrix effect of USY based FCC catalyst (After steaming) on product yield for vacuum gas oil (VGO) cracking at 550 °C.

Name of catalyst	St-Y01	St-Y02	St-Y03	St-Y04	St-Y05
Catalyst/Oil (g/g)	2.81	2.76	2.75	2.71	2.78
Mass balance	101	103.2	101.8	100.1	97.8
Conversion (%)	76.90	76.96	77.84	78.87	81.44
Product Yields (wt. %)					
H_2	0.07	0.06	0.06	0.06	0.06
C_1	0.89	0.79	0.89	0.98	1.07
C_2	0.97	0.81	0.97	1.04	1.08
C_2=	1.57	1.31	1.79	1.64	1.67
C_3	1.17	1.09	1.60	1.49	1.62
C_3=	7.12	6.75	7.82	7.25	7.31
iC_4	4.62	5.85	5.62	5.71	6.03
nC_4	0.87	2.11	1.09	1.16	1.29
T_2C_4=	2.53	2.20	2.36	2.39	2.34
$1C_4$=	1.95	1.72	1.82	1.86	1.83
iC_4=	2.03	1.67	1.88	1.55	1.41
C_2C_4=	2.04	1.76	1.88	1.90	1.87
C_4=(Liq.)	0.39	0.86	0.64	0.82	0.85
Total Gas	26.59	27.32	28.60	28.08	29.03
Gasoline	48.66	47.81	46.96	48.30	49.38
LCO	14.80	14.79	14.27	13.95	12.62
HCO	8.29	8.25	7.89	7.18	5.94
Coke	1.65	1.83	2.28	2.50	3.03
H_2-C_2 (dry gas)	3.51	2.96	3.70	3.72	3.87
C_3-C_4 (LPG)	23.08	24.36	24.90	24.35	25.16
C_2=-C_4= (Light olefins)	18.00	16.61	18.37	17.63	17.89
	Selectivity (yield/conversion × 100) %				
Gasoline	63.3	62.1	60.3	61.2	60.6
LCO	19.2	19.2	18.3	17.7	15.5
HCO	10.8	10.7	10.1	9.1	7.3
Coke	2.1	2.4	2.9	3.2	3.7
LPG	30.0	31.6	32.0	30.9	30.9
Light olefins	23.4	21.6	23.6	22.4	22.0
Dry gas	4.56	3.85	4.76	4.72	4.75

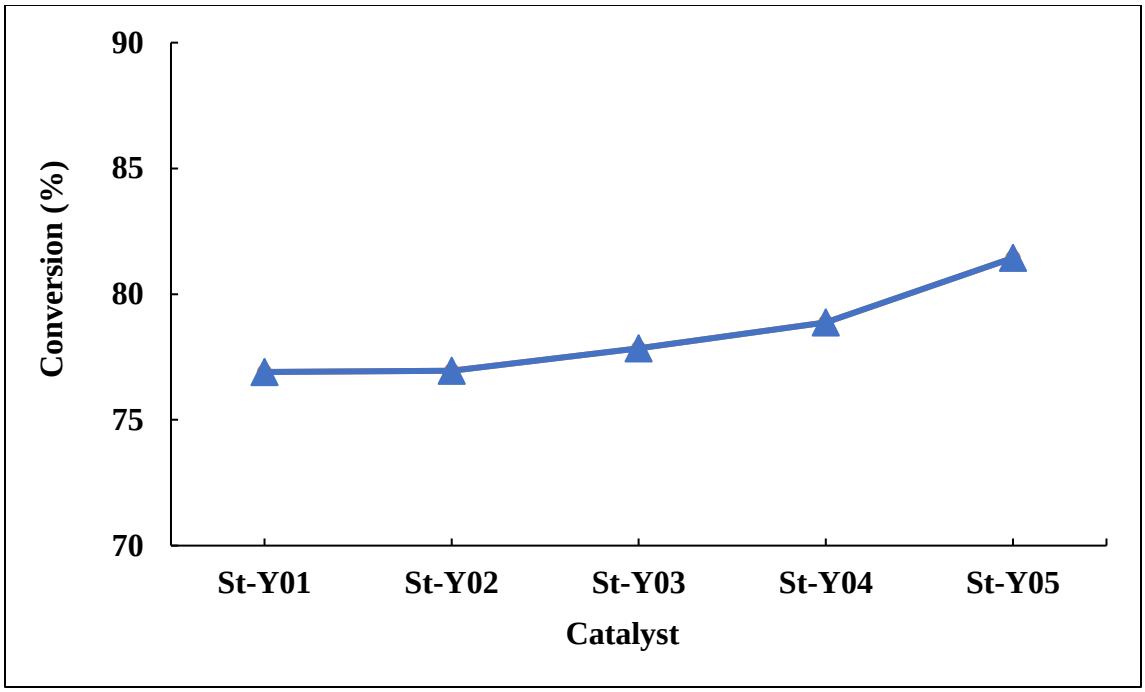

Figure 4.10: Conversion (%) of steamed catalysts for different Zeolite/Matrix (%).

The effect of steamed FCC catalyst samples on gasoline selectivity as a function of zeolite to matrix ratio is shown in Figure 4.11. It is observed that gasoline selectivity decreases with an increase in zeolite to matrix ratio. This behaviour is expected due to the over-cracking of gasoline at a high zeolite to matrix ratio. Gasoline selectivity for steamed FCC catalysts was found to be St-Y01 (63%), St-Y02 (62%), St-Y03 (60%), St-Y04 (61%), and St-Y05 (60%). The percentage decrease of gasoline selectivity was 4.7% for an increase in zeolite to matrix ratio of 18 to 50. The decrease in gasoline selectivity because of an increase in zeolite to matrix ratio was associated with an increase in LPG selectivity. For a 4.7% drop in gasoline selectivity for steamed FCC catalyst samples, a 3% increase in selectivity of LPG was obtained. Like the gasoline trend, LCO and HCO selectivity was found to decrease with an increase in zeolite to matrix ratio for steamed FCC catalyst samples. This behaviour is due to an increase in cracking rates of LCO and HCO as

conversion increases. The trend of LCO and HCO selectivity as a function of zeolite to matrix ratio are shown in Figure 4.12. For steamed FCC samples, a 7% decrease in LCO selectivity for zeolite to matrix ratio of 18 to 35, while a 12% drop was noted for zeolite to matrix ratio of 35 to 50. On the other hand, a decrease in HCO selectivity was 15% for zeolites to matrix ratio of 18 to 35 as compared to a 19% drop for zeolite to matrix ratio 35 to 50. The combined selectivity of gasoline and LCO for St-Y01 is reported 82% as compared to 76% for St-Y05. It can be observed that zeolite to matrix ratio of 15 had the highest combined selectivity of gasoline and LCO for steamed catalysts due to less over-cracking of LCO and gasoline.

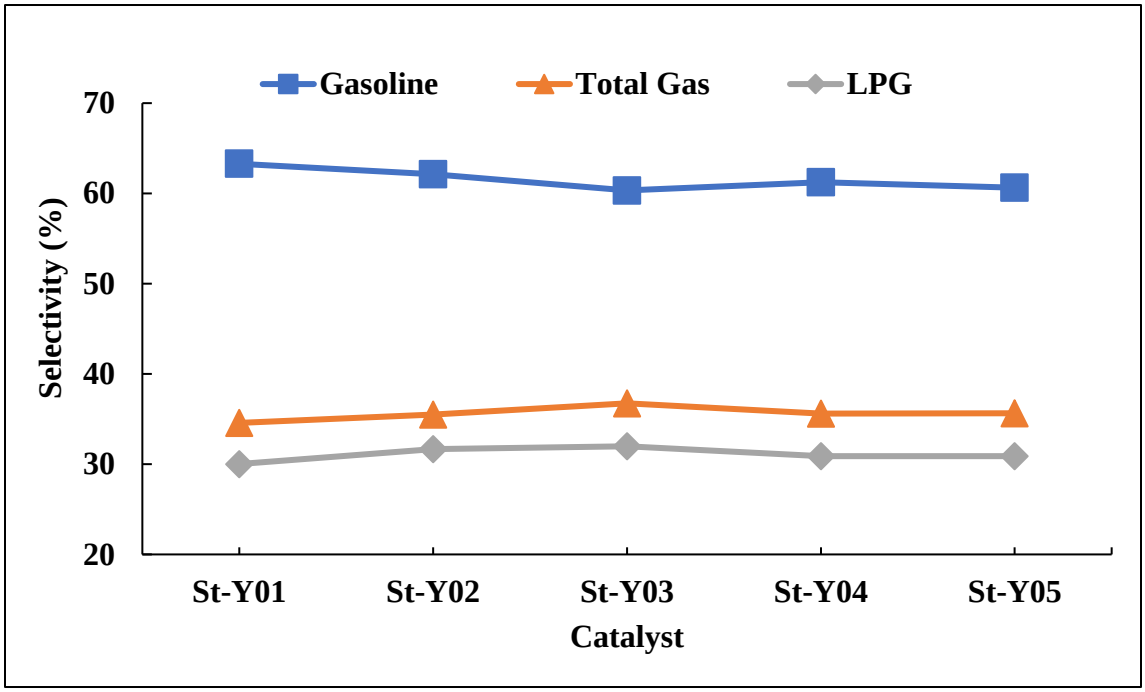

Figure 4.11: Gasoline, Total Gas, and LPG selectivity (%) of steamed catalysts for different Zeolite/Matrix (%).

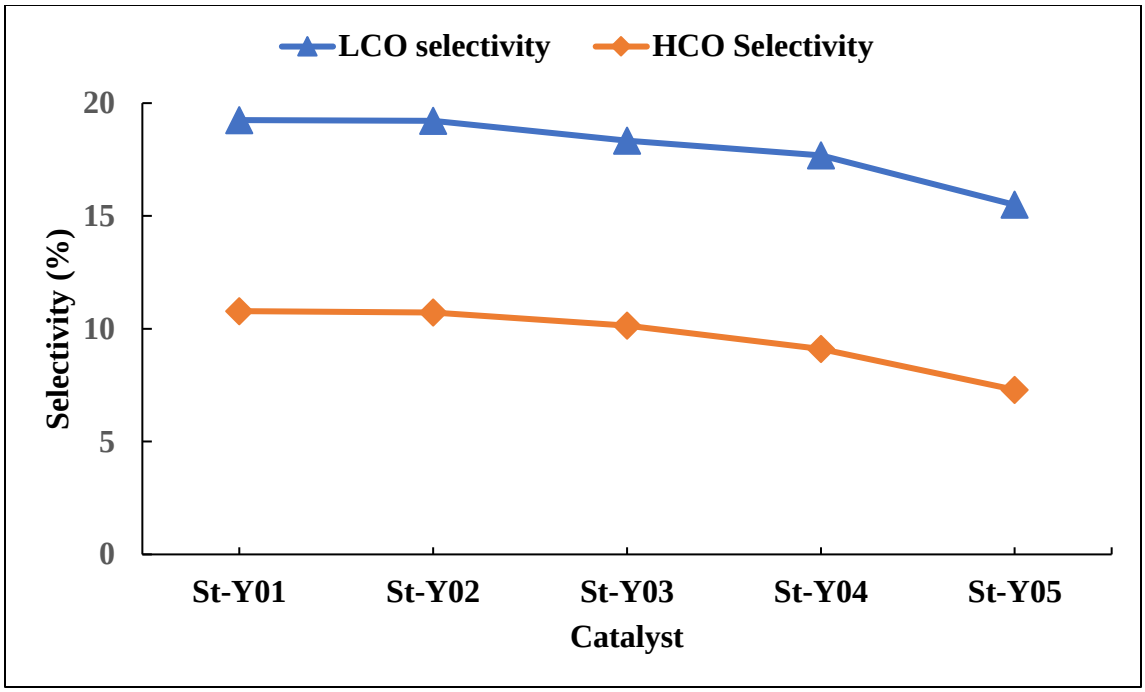

Figure 4.12: LCO and HCO selectivity (%) of steamed catalysts for different Zeolite/Matrix (%).

In general, as conversion increases, yields of light cycle oil (LCO) and gasoline pass through maxima and then decrease while HCO declines and dry gas and coke yields increase steeply. The optimum conversion reported in the literature is 70-75%, and above 76% conversion is reported in the present study for all steamed FCC catalysts. As such, the trends of decreasing gasoline, LCO, and HCO selectivity are in good agreement with the literature [86].

Similar to LPG, coke selectivity was indicated to increase with an increase in zeolite to matrix ratio and VGO conversion. Figure 4.13 demonstrates the effect of zeolite to matrix ratio on coke selectivity. FCC catalyst samples containing high zeolite to matrix ratio produce more coke as compared to low zeolite to matrix ratio. Steamed FCC catalyst St-Y01 gave only 2.1% coke selectivity, while 3.7% coke selectivity was observed in the St-

Y05 sample. Overall, a 76% relative increase in coke selectivity was observed from St-Y01 to St-Y05.

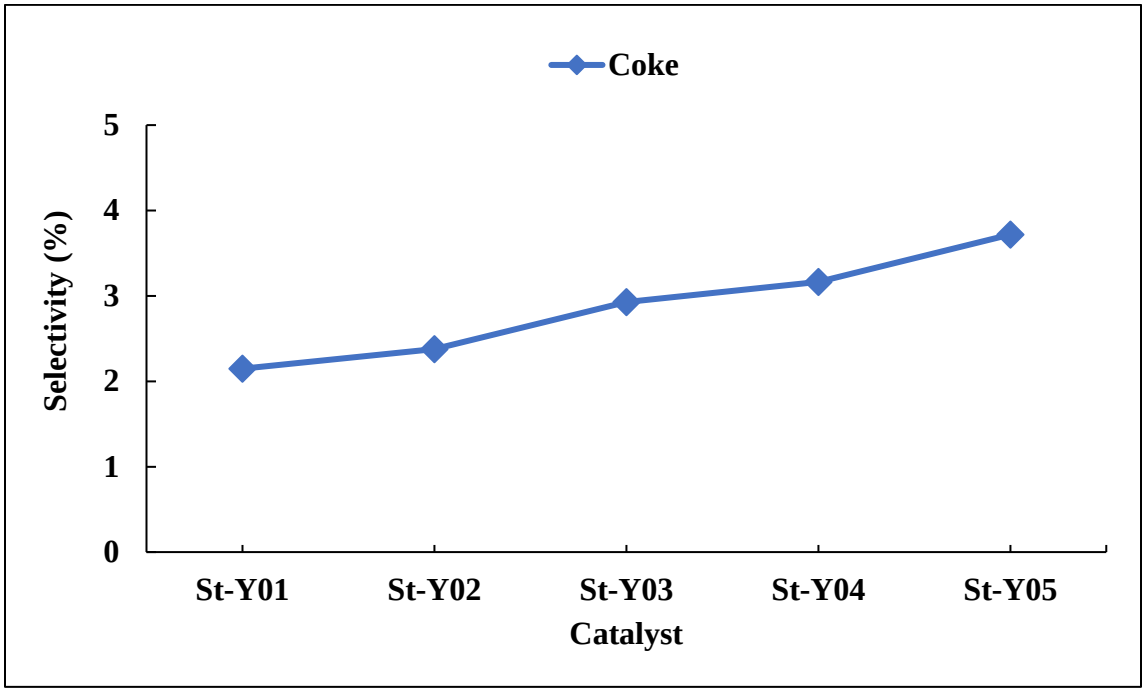

Figure 4.13: Coke selectivity (%) of steamed catalysts for different Zeolite/Matrix (%).

4.5 Evaluation and comparison of modified Y-zeolite based FCC catalysts with USY based FCC catalysts

Steam deactivated FCC catalyst samples were used for the catalytic cracking of VGO as feed in a microactivity unit. The distribution of product yields as a result of catalytic cracking on the steamed base catalyst (St-Y01) and steamed modified catalysts (St-MY30, St-MY73, and St-MY120) are shown in Table 4.5. The base catalyst (St-Y01) having a zeolite to matrix ratio of 18 used for the comparison purposes due to its high gasoline as well as low coke selectivity (%).

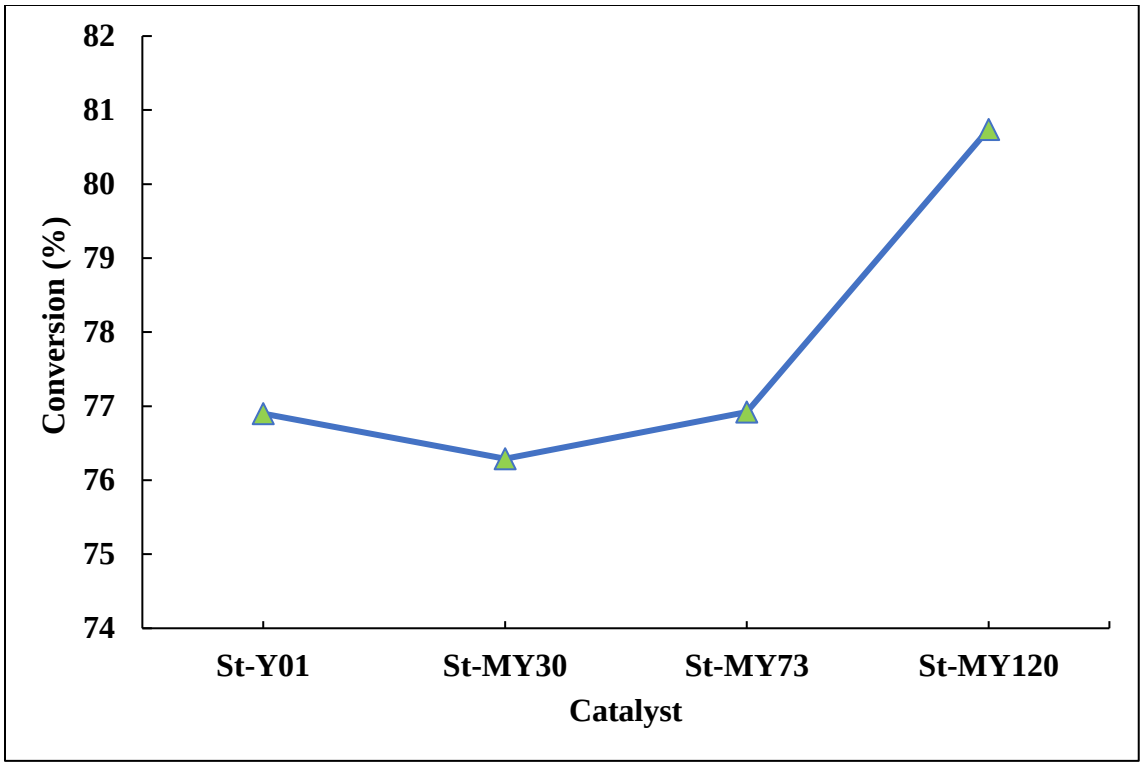

Figure 4.14: Conversion (%) of base (St-Y01) and modified FCC catalyst (St-MY30, St-MY73, and St-MY120).

From Table 4.5, it is noted that vacuum gas oil conversion increased from 76.9% (base catalyst) to 80.7% (mesoporous catalyst) at 550ºC. It is noted that the first three catalysts including base (St-Y01) and modified (MY30, MY73) have 76% conversion, while for MY120, 80% conversion was achieved. Figure 4.14 shows the trend of increasing conversion (%) for the base and modified FCC catalysts.

Table 4.5. Comparative MAT data of base catalyst and modified zeolite-based FCC catalysts (both steamed at 750 °C) for vacuum gas oil (VGO) cracking at 550 °C.

Name of catalyst	St-Y01	St-MY30	St-MY73	St-MY120
Catalyst/Oil (g/g)	2.81	2.89	2.89	2.78
Mass balance	101	101.8	100.3	102.8
Conversion (%)	76.90	76.29	76.92	80.74
Product Yields (wt. %)				
H_2	0.07	0.07	0.06	0.07
C_1	0.89	0.85	0.72	0.89
C_2	0.97	0.88	0.76	0.96
C_2=	1.57	1.46	1.24	1.52
C_3	1.17	1.32	1.01	1.25
C_3=	7.12	7.04	6.61	6.97
iC_4	4.62	5.61	4.75	5.43
nC_4	0.87	1.05	0.82	0.99
T_2C_4=	2.53	2.34	2.36	2.41
$1C_4$=	1.95	1.84	1.87	1.90
iC_4=	2.03	1.74	2.02	1.67
C_2C_4=	2.04	1.86	1.87	1.91
C_4=(Liq.)	0.39	0.80	1.05	1.05
Total Gas	26.59	26.87	25.14	27.03
Gasoline	48.66	47.48	50.37	52.00
LCO	14.80	15.85	15.52	14.49
HCO	8.29	7.86	7.56	4.77
Coke	1.65	1.94	1.41	1.71
H_2-C_2 (dry gas)	3.51	3.26	2.78	3.44
C_3-C_4 (LPG)	23.08	23.61	22.36	23.58
C_2=-C_4= (Light olefins)	18.00	17.10	17.02	17.44
	Selectivity (yield/conversion × 100) %			
Gasoline	63.27	62.23	65.48	64.40
LCO	19.24	20.77	20.17	17.94
HCO	10.78	10.30	9.82	5.90
Coke	2.14	2.54	1.83	2.11
LPG	30.01	30.94	29.06	29.20
Light olefins	23.40	22.41	22.12	21.60
Dry gas	4.56	4.27	3.61	4.26

From Table 4.5, it is shown that the highest gasoline selectivity of 65% was achieved for St-MY73 as compared to 63% for St-Y01. On the other hand, 62% and 64% of gasoline selectivity were obtained for St-MY30 and St-MY120. LCO selectivity (%) was decreased for St-MY120 as compared to St-Y01, whereas it increases for St-MY30 and St-MY73. On the other hand, HCO selectivity (%) decreases from St-Y01 to St-MY120. It is worth noting that HCO yield was significantly decreased for St-MY120 as compared to St-Y01. For instance, it was 10% and 5% for St-Y01 and St-MY120, respectively. Similarly, 10% and 9% HCO selectivity (%) was noted for St-MY30 and St-MY73, respectively. From Table 4.6, the relative difference of gasoline selectivity was +3.4% and +1.7% for St-MY73 and St-MY120, respectively, whereas +4.8% and -6.7% was noted as a relative difference of LCO selectivity as compared to St-Y01 (base catalyst). Similarly, -8.9% and -45.2% relative difference was observed for HCO selectivity. Figure 4.15 demonstrates the selectivity (%) of gasoline, LCO, HCO, and coke for all the deactivated catalysts.

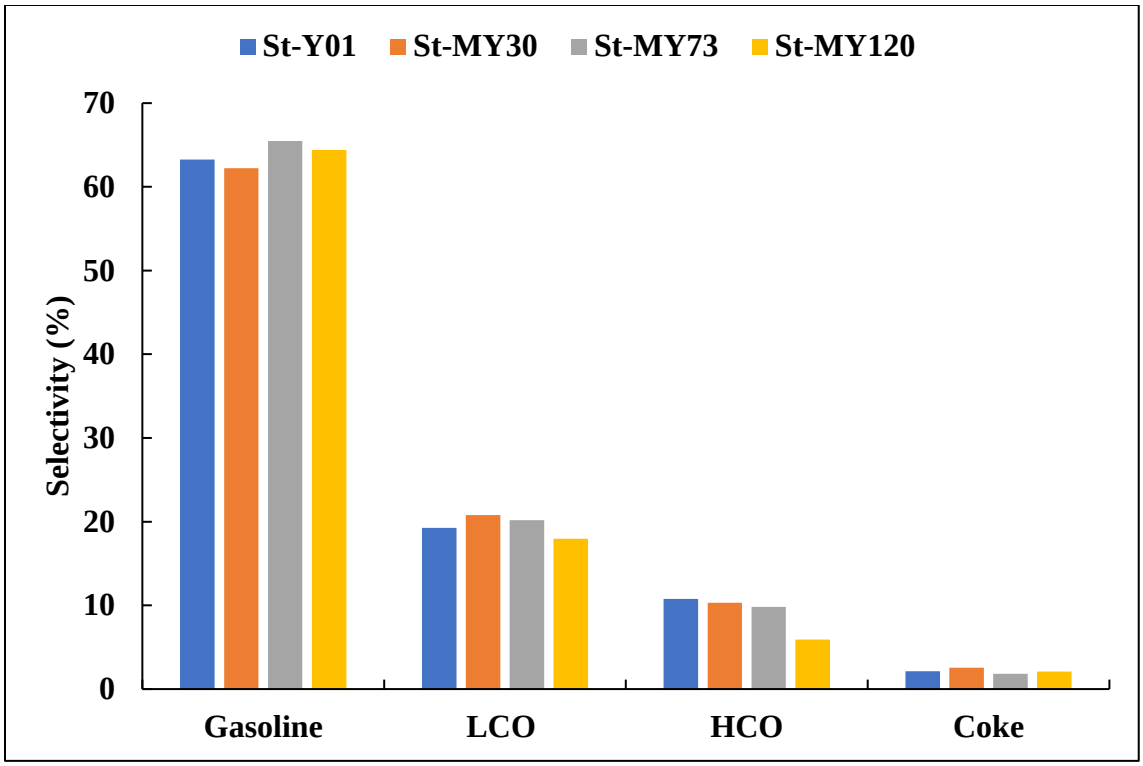

Figure 4.15. Selectivity (%) of gasoline, LCO, HCO, and coke for base (St-Y01) and modified FCC catalysts (St-MY30, St-MY73, and St-MY120).

Table 4.6. Relative difference (%) of modified zeolite products with St-Y01 (base catalyst) on selectivity bases.

Products	St-MY30	St-MY73	St-MY120
Gasoline	-1.64	+3.49	+1.79
LCO	+7.95	+4.83	-6.76
HCO	-4.45	-8.91	-45.27
Coke	+18.69	-14.49	-1.40
Dry gas	-6.36	-20.83	-6.58

Moreover, coke selectivity (%) is lie in between 1% and 3% for all modified catalysts as well as base catalyst (St-Y01). St-MY73 has a significant relative difference of -14.4% in coke selectivity while for St-MY120 it was -1.4% as compared to the base catalyst (St-

Y01). However, the highest conversion was obtained for St-MY120 as compared to the base catalyst but still, coke yield is almost similar to the base catalyst (St-Y01). As we know that with the increase in conversion (%), coke yield (%) should be increased. But similar coke yield achieved by an increase in conversion could be due to the mesoporous structure created into the zeolite structure that reduced the diffusion limitations in the post-treated conventional zeolite [70]. St-MY73 and St-MY120 give high gasoline and less HCO selectivity as compared to the base catalyst (St-Y01) due to the mesoporosity inside the zeolite which allows the large molecules (heavy cycle oil) from the feedstock to approach the acidic sites inside the zeolite structure. Similarly, less coke and dry gases in MY73 and MY120 support the concept of ease in the diffusion of the reactants as well as products into and out of the zeolite crystals to impede the undesirable secondary reactions such as over cracking of gasoline.

CHAPTER 5

CONCLUSION & RECOMMENDATION

5.1 Conclusion

The main objective of this study was the synthesis of the FCC catalyst using mesoporous Y-zeolite to enhance the gasoline selectivity and reduce the coke selectivity. From XRD analysis, it was concluded that the generation of mesoporosity causes an expected decrease of XRD peaks intensity due to the formation of mesopores without the presence of the amorphous material. From N_2 physisorption, it is noted that micropore volume decreases with an increase in acid concentration for MY30, MY73, and MY120 samples, while substantial increase of mesopore volume was observed. For MY73 and MY120, mesopore volume was 0.16 cc/g and 0.30 cc/g as compared to 0.03 cc/g for parent zeolite (Na-Y zeolite). The modification has caused an increase of silica to alumina ratio in modified Y-zeolites from 5.6 to 9.3. For modified zeolites, a bimodal pore size distribution was also observed which enhances the accessibility of active sites and reduces the diffusion limitations of heavy molecules in heterogeneous catalysis reactions. From NH_3-TPD method, it is noted that the acidity of the modified zeolite samples decreases as the dealumination increases from sample MY30 to MY120. MY30 has a total acidity of 0.724 mmol/g, whereas 0.700 and 0.578 mmol/g was observed for MY73 and MY120 respectively. All modified zeolite samples were used for the preparation of FCC catalysts. The characterization data of modified Y zeolite-based FCC catalysts show a 26% decrease in micropore volume and a 17% increase in mesopore volume for St-MY120 as compared to St-MY30. In the series of five steamed FCC catalyst samples with different zeolite to

matrix ratio, VGO conversion was increased from 76% to 81% with an increase in zeolite to matrix ratio. The surface area and acidity of all FCC catalyst samples were found to increase as the zeolite to matrix ratio increases. At a low zeolite to matrix ratio of 18, maximum gasoline and LCO selectivity was achieved with minimum gas and coke selectivity. Based on high gasoline and less coke selectivity, USY based FCC catalyst with zeolite to matrix ratio of 18 was chosen for comparison with modified Y-zeolite based FCC catalysts. MAT unit testing of FCC catalysts made from mesoporous Y-zeolite indicates the improved selectivity of products i.e. high selectivity of gasoline and LCO, and low coke, HCO, and dry gases. The relative difference of gasoline selectivity was +3.4% and +1.7% for St-MY73 and St-MY120, respectively, whereas +4.8% and -6.7% was noted as a relative difference of LCO selectivity as compared to St-Y01 (base catalyst). Similarly, -8.9% and -45.2% relative difference of HCO was observed for St-MY73 and St-MY120, respectively. It is noted that St-MY73 has a significant relative difference of -14.4% in coke, while for St-MY120, it was -1.4% as compared to the base catalyst (St-Y01). St-MY73 was performed better based on gasoline, LCO, and coke selectivity.

5.2 Recommendations

The following are recommended for further research work:

- Use of different synthesis methods for mesoporosity creation other than post-treatment of Y-zeolite such as templating method adopting a bottom-up approach because of the retention of microporous volume as well as the acidity of the zeolite
- Preparation of FCC catalyst using spray dryer to achieve suitable pellet size (50 – 90 μm) to assess the performance close to commercial conditions
- Addition of HZSM-5 in mesoporous Y-zeolite based FCC catalysts for the enhancement in propylene selectivity

REFERENCES

[1] R.J.G.P.P. Sadeghbeigi, Houston, Fluid Catalytic Cracking Handbook Design, Operation and Troubleshouting of FCC facilities, 2 (2000) 234-275.

[2] J.H. Gary, G.E. Handwerk, M.J. Kaiser, Petroleum refining: technology and economics, CRC press, 2007.

[3] J. Zhu, X. Meng, F. Xiao, Mesoporous zeolites as efficient catalysts for oil refining and natural gas conversion, Frontiers of Chemical Science and Engineering, 7 (2013) 233-248.

[4] E. Vogt, B. Weckhuysen, Fluid catalytic cracking: recent developments on the grand old lady of zeolite catalysis, Chemical Society Reviews, 44 (2015) 7342-7370.

[5] X. Chen, I. Grossmann, L. Zheng, A comparative study of continuous-time models for scheduling of crude oil operations in inland refineries, Computers & Chemical Engineering, 44 (2012) 141-167.

[6] L.A. Hadidi, A.S. AlDosary, A.K. Al-Matar, O.A. Mudallah, An optimization model to improve gas emission mitigation in oil refineries, Journal of cleaner production, 118 (2016) 29-36.

[7] J. Hou, X. Li, H. Sui, The optimization and prediction of properties for crude oil blending, Computers & Chemical Engineering, 76 (2015) 21-26.

[8] E. Sa'idi, B. Anvaripour, F. Jaderi, N. Nabhani, Fuzzy risk modeling of process operations in the oil and gas refineries, Journal of Loss Prevention in the Process Industries, 30 (2014) 63-73.

[9] M.H. Ahmed, O. Muraza, Stability Assessment of Regenerated Hierarchical ZSM-48 Zeolite Designed by Post-Synthesis Treatment for Catalytic Cracking of Light Naphtha, Energy & fuels, 31 (2017) 14097-14103.

[10] A. Galadima, O. Muraza, Stability improvement of zeolite catalysts under hydrothermal conditions for their potential applications in biomass valorization and crude oil upgrading, Microporous and Mesoporous Materials, 249 (2017) 42-54.

[11] A.K. Jamil, O. Muraza, M.H. Ahmed, A. Zainalabdeen, K. Muramoto, Y. Nakasaka, Z.H. Yamani, T. Yoshikawa, T. Masuda, Hydrothermally stable acid-modified ZSM-22 zeolite for selective propylene production via steam-assisted catalytic cracking of n-hexane, Microporous and Mesoporous Materials, 260 (2018) 30-39.

[12] J.N. Armor, New catalytic technology commercialized in the USA during the 1980's, Applied catalysis, 78 (1991) 141-173.

[13] R. Argauer, G. Landolt, US Pat., 3702886, (1976).

[14] J. Biswas, I. Maxwell, Recent process-and catalyst-related developments in fluid catalytic cracking, Applied Catalysis, 63 (1990) 197-258.

[15] M.E. Davis, Ordered porous materials for emerging applications, Nature, 417 (2002) 813.

[16] J. Čejka, S. Mintova, Perspectives of micro/mesoporous composites in catalysis, Catalysis Reviews, 49 (2007) 457-509.

[17] M. Choi, K. Na, J. Kim, Y. Sakamoto, O. Terasaki, R. Ryoo, Stable single-unit-cell nanosheets of zeolite MFI as active and long-lived catalysts, Nature, 461 (2009) 246.

[18] X. Meng, F. Nawaz, F.-S. Xiao, Templating route for synthesizing mesoporous zeolites with improved catalytic properties, Nano Today, 4 (2009) 292-301.

[19] J. Pérez-Ramírez, C.H. Christensen, K. Egeblad, C.H. Christensen, J.C. Groen, Hierarchical zeolites: enhanced utilisation of microporous crystals in catalysis by advances in materials design, Chemical Society Reviews, 37 (2008) 2530-2542.

[20] C.H. Christensen, K. Johannsen, I. Schmidt, C.H. Christensen, Catalytic benzene alkylation over mesoporous zeolite single crystals: improving activity and selectivity with

a new family of porous materials, Journal of the american chemical society, 125 (2003) 13370-13371.

[21] B. Liu, Q. Duan, C. Li, Z. Zhu, H. Xi, Y. Qian, Template synthesis of the hierarchically structured MFI zeolite with nanosheet frameworks and tailored structure, New Journal of Chemistry, 38 (2014) 4380-4387.

[22] G.J.d.A. Soler-Illia, C. Sanchez, B. Lebeau, J. Patarin, Chemical strategies to design textured materials: from microporous and mesoporous oxides to nanonetworks and hierarchical structures, Chemical reviews, 102 (2002) 4093-4138.

[23] R. Srivastava, M. Choi, R. Ryoo, Mesoporous materials with zeolite framework: remarkable effect of the hierarchical structure for retardation of catalyst deactivation, Chemical Communications, (2006) 4489-4491.

[24] C. Mei, Z. Liu, P. Wen, Z. Xie, W. Hua, Z. Gao, Regular HZSM-5 microboxes prepared via a mild alkaline treatment, Journal of Materials Chemistry, 18 (2008) 3496-3500.

[25] J. Pérez-Ramírez, S. Abelló, L.A. Villaescusa, A. Bonilla, Toward Functional Clathrasils: Size-and Composition-Controlled Octadecasil Nanocrystals by Desilication, Angewandte Chemie, 120 (2008) 8031-8035.

[26] J. Zhou, Z. Hua, J. Zhao, Z. Gao, S. Zeng, J. Shi, A micro/mesoporous aluminosilicate: key factors affecting framework crystallization during steam-assisted synthesis and its catalytic property, Journal of Materials Chemistry, 20 (2010) 6764-6771.

[27] H. Li, H. Wu, J.-l. Shi, Competition balance between mesoporous self-assembly and crystallization of zeolite: a key to the formation of mesoporous zeolite, Journal of Alloys and Compounds, 556 (2013) 71-78.

[28] P. Losch, T.C. Hoff, J.F. Kolb, C. Bernardon, J.-P. Tessonnier, B.J.C. Louis, Mesoporous ZSM-5 zeolites in acid catalysis: top-down vs. bottom-up approach, 7 (2017) 225.

[29] M.-C. Silaghi, C. Chizallet, P.J.M. Raybaud, M. Materials, Challenges on molecular aspects of dealumination and desilication of zeolites, 191 (2014) 82-96.

[30] K. Li, J. Valla, J.J.C. Garcia-Martinez, Realizing the commercial potential of hierarchical zeolites: new opportunities in catalytic cracking, 6 (2014) 46-66.

[31] V. Valtchev, G. Majano, S. Mintova, J.J.C.S.R. Pérez-Ramírez, Tailored crystalline microporous materials by post-synthesis modification, 42 (2013) 263-290.

[32] A. Sachse, A. Grau-Atienza, E.O. Jardim, N. Linares, M. Thommes, J.J.C.G. Garcia-Martinez, Design, Development of intracrystalline mesoporosity in zeolites through surfactant-templating, 17 (2017) 4289-4305.

[33] A. Al-Ani, J.J. Haslam, N.E. Mordvinova, O.I. Lebedev, A. Vicente, C. Fernandez, V.J.N.A. Zholobenko, Synthesis of nanostructured catalysts by surfactant-templating of large-pore zeolites, 1 (2019) 2029-2039.

[34] M.L. Occelli, Fluid Catalytic Cracking VII:: Materials, Methods and Process Innovations, Elsevier, 2011.

[35] A. Talebian-Kiakalaieh, S.J.J.o.I. Tarighi, E. Chemistry, Synthesis of hierarchical Y and ZSM-5 zeolites using post-treatment approach to maximize catalytic cracking performance, (2020).

[36] J. Scherzer, Octane-enhancing Zeolite FCC: Scientific and Technical Aspects, in, Marcel-Dekker. New York, NY, 1990.

[37] J. de Jong, Ketjen Catalyst Symposium 1986, Scheveningen, The Netherlands, Paper F-2.

[38] J. Magee, M. Mitchell Jr, Instrumental methods of FCC catalyst characterization, Fluid Catalytic Cracking: Science and Technology, (1993) 183.

[39] M.L. Occelli, P. O'Connor, Fluid catalytic cracking III, American Chemical Society, 1994.

[40] J. Scherzer, Octane-enhancing, zeolitic FCC catalysts: scientific and technical aspects, Catalysis Reviews—Science and Engineering, 31 (1989) 215-354.

[41] A. Corma, F. Mocholi, New silica-alumina-magnesia FCC active matrix and its possibilities as a basic nitrogen passivating compound, Applied Catalysis A: General, 84 (1992) 31-46.

[42] M. Falco, E. Morgado, N. Amadeo, U. Sedran, Accessibility in alumina matrices of FCC catalysts, Applied Catalysis A: General, 315 (2006) 29-34.

[43] N. Kubicek, F. Vaudry, B. Chiche, P. Hudec, F. Di Renzo, P. Schulz, F. Fajula, Stabilization of zeolite beta for fcc application by embedding in amorphous matrix, Applied Catalysis A: General, 175 (1998) 159-171.

[44] A. Lappas, D. Iatridis, M. Papapetrou, E. Kopalidou, I. Vasalos, Feedstock and catalyst effects in fluid catalytic cracking–Comparative yields in bench scale and pilot plant reactors, Chemical Engineering Journal, 278 (2015) 140-149.

[45] E. Moorehead, J. McLean, W. Cronkright, Microactivity evaluation of FCC catalysts in the laboratory: principles, approaches and applications, in: Studies in Surface Science and Catalysis, Elsevier, 1993, pp. 223-255.

[46] A. Hussain, A. Aitani, M. Kubů, J. Čejka, S. Al-Khattaf, Catalytic cracking of Arabian Light VGO over novel zeolites as FCC catalyst additives for maximizing propylene yield, Fuel, 167 (2016) 226-239.

[47] J.H. Gary, G.E. Handwerk, Petroleum Refining: Technology and Economics, New York: M, in, Dekker, 1994.

[48] X. Dupain, M. Makkee, J. Moulijn, Optimal conditions in fluid catalytic cracking: A mechanistic approach, Applied Catalysis A: General, 297 (2006) 198-219.

[49] A. Corma, J. Planelles, J. Sanchez-Marin, F. Tomas, The role of different types of acid site in the cracking of alkanes on zeolite catalysts, Journal of Catalysis, 93 (1985) 30-37.

[50] B. Greensfelder, H. Voge, G. Good, Catalytic and thermal cracking of pure hydrocarbons: Mechanisms of Reaction, Industrial & Engineering Chemistry, 41 (1949) 2573-2584.

[51] A. Corma, A. Orchillés, Current views on the mechanism of catalytic cracking, Microporous and mesoporous materials, 35 (2000) 21-30.

[52] S. Kotrel, H. Knözinger, B. Gates, The Haag–Dessau mechanism of protolytic cracking of alkanes, Microporous and Mesoporous Materials, 35 (2000) 11-20.

[53] J. Weitkamp, Zeolites and catalysis, Solid State Ionics, 131 (2000) 175-188.

[54] M. Hartmann, A.G. Machoke, W. Schwieger, Catalytic test reactions for the evaluation of hierarchical zeolites, Chemical Society Reviews, 45 (2016) 3313-3330.

[55] D. Serrano, P. Pizarro, Synthesis strategies in the search for hierarchical zeolites, Chemical Society Reviews, 42 (2013) 4004-4035.

[56] H.G. Karge, J. Weitkamp, Molecular sieves, Science and Technology, 1 (1999).

[57] A. Feliczak-Guzik, Hierarchical zeolites: synthesis and catalytic properties, Microporous and Mesoporous Materials, 259 (2018) 33-45.

[58] C.S. Triantafillidis, A.G. Vlessidis, N.P. Evmiridis, Dealuminated H− Y zeolites: influence of the degree and the type of dealumination method on the structural and acidic characteristics of H− Y zeolites, Industrial & engineering chemistry research, 39 (2000) 307-319.

[59] C.J. Van Oers, W.J. Stevens, E. Bruijn, M. Mertens, O.I. Lebedev, G. Van Tendeloo, V. Meynen, P. Cool, Formation of a combined micro-and mesoporous material using zeolite Beta nanoparticles, Microporous and Mesoporous Materials, 120 (2009) 29-34.

[60] M.S. Holm, E. Taarning, K. Egeblad, C.H. Christensen, Catalysis with hierarchical zeolites, Catalysis Today, 168 (2011) 3-16.

[61] Z. Qin, W. Shen, S. Zhou, Y. Shen, C. Li, P. Zeng, B.J.M. Shen, M. Materials, Defect-assisted mesopore formation during Y zeolite dealumination: The types of defect matter, (2020) 110248.

[62] E. Koohsaryan, M. Anbia, Nanosized and hierarchical zeolites: A short review, Chinese Journal of Catalysis, 37 (2016) 447-467.

[63] J. Groen, L. Peffer, J. Moulijn, J. Pérez-Ramírez, M. Ogura, S.-Y. Shinomiya, J. Tateno, Y. Nara, E. Kikuchi, M. Matsukata, Chem. Lett, 29 (2000) 882-883.

[64] T. Suzuki, T. Okuhara, Change in pore structure of MFI zeolite by treatment with NaOH aqueous solution, Microporous and mesoporous materials, 43 (2001) 83-89.

[65] R. Zhang, D. Raja, Y. Zhang, Y. Yan, A.A. Garforth, Y. Jiao, X.J.T.i.C. Fan, Sequential Microwave-Assisted Dealumination and Hydrothermal Alkaline Treatments of Y Zeolite for Preparing Hierarchical Mesoporous Zeolite Catalysts, (2020) 1-11.

[66] B. Meng, S. Ren, Z. Li, H. Duan, X. Gao, H. Zhang, W. Song, Q. Guo, B.J.A.A.N.M. Shen, Intra-Crystalline Mesoporous Zeolite [Al, Zr]-Y for Catalytic Cracking, (2020).

[67] B. Meng, S. Ren, X. Liu, L. Zhang, Q. Hu, J. Wang, Q. Guo, B.J.I. Shen, E.C. Research, Synthesis of USY Zeolite with a High Mesoporous Content by Introducing Sn and Enhanced Catalytic Performance, 59 (2020) 5712-5719.

[68] V. Valtchev, E. Balanzat, V. Mavrodinova, I. Diaz, J. El Fallah, J.-M. Goupil, High energy ion irradiation-induced ordered macropores in zeolite crystals, Journal of the American Chemical Society, 133 (2011) 18950-18956.

[69] D. Verboekend, J. Pérez-Ramírez, Design of hierarchical zeolite catalysts by desilication, Catalysis Science & Technology, 1 (2011) 879-890.

[70] J. García-Martínez, M. Johnson, J. Valla, K. Li, J.Y.J.C.S. Ying, Technology, Mesostructured zeolite Y—high hydrothermal stability and superior FCC catalytic performance, 2 (2012) 987-994.

[71] B. Speronello, J. Garcia-Martinez, A. Hanson, R.J.R.O. Hu, FCC catalysts with mesoporous zeolite yield higher quality products, 2 (2011).

[72] K. Na, M. Choi, R. Ryoo, Recent advances in the synthesis of hierarchically nanoporous zeolites, Microporous and Mesoporous Materials, 166 (2013) 3-19.

[73] P. Lv, L. Yan, Y. Liu, M. Wang, W. Bao, F.J.I. Li, E.C. Research, Catalytic upgrading of coal pyrolysis gaseous tar over hierarchical Y-type zeolites synthesized using a microwave hydrothermal method, 58 (2019) 21817-21826.

[74] H. Wang, T.J. Pinnavaia, MFI zeolite with small and uniform intracrystal mesopores, Angewandte Chemie International Edition, 45 (2006) 7603-7606.

[75] Y. Fang, H. Hu, An ordered mesoporous aluminosilicate with completely crystalline zeolite wall structure, Journal of the American Chemical Society, 128 (2006) 10636-10637.

[76] H. Chen, J. Wydra, X. Zhang, P.-S. Lee, Z. Wang, W. Fan, M. Tsapatsis, Hydrothermal synthesis of zeolites with three-dimensionally ordered mesoporous-imprinted structure, Journal of the American Chemical Society, 133 (2011) 12390-12393.

[77] M. Kustova, K. Egeblad, K. Zhu, C.H. Christensen, Versatile route to zeolite single crystals with controlled mesoporosity: in situ sugar decomposition for templating of hierarchical zeolites, Chemistry of materials, 19 (2007) 2915-2917.

[78] J. Scherzer, Octane-enhancing zeolitic FCC catalysts: scientific and technical aspects, CRC Press, 1990.

[79] A. Al-Ani, R.J. Darton, S. Sneddon, V.J.A.A.N.M. Zholobenko, Nanostructured Zeolites: The introduction of intracrystalline mesoporosity in basic faujasite-type catalysts, 1 (2017) 310-318.

[80] D. Serrano, R. Sanz, R. Garcia, A. Peral, I. Moreno, M.J.N.J.o.C. Linares, Hierarchical ZSM-5 zeolite with uniform mesopores and improved catalytic properties, 40 (2016) 4206-4216.

[81] K.A. Cychosz, R. Guillet-Nicolas, J. García-Martínez, M.J.C.S.R. Thommes, Recent advances in the textural characterization of hierarchically structured nanoporous materials, 46 (2017) 389-414.

[82] E.P. Barrett, L.G. Joyner, P.P.J.J.o.t.A.C.s. Halenda, The determination of pore volume and area distributions in porous substances. I. Computations from nitrogen isotherms, 73 (1951) 373-380.

[83] N. Linares, E.O. Jardim, A. Sachse, E. Serrano, J.J.A.C. García-Martínez, The Energetics of Surfactant-Templating of Zeolites, 130 (2018) 8860-8864.

[84] J.C. Groen, J.C. Jansen, J.A. Moulijn, J.J.T.J.o.P.C.B. Pérez-Ramírez, Optimal aluminum-assisted mesoporosity development in MFI zeolites by desilication, 108 (2004) 13062-13065.

[85] M.M. Treacy, J.B. Higgins, Collection of simulated XRD powder patterns for zeolites fifth (5th) revised edition, Elsevier, 2007.

[86] C.H. Bartholomew, M.D. Argyle, Advances in catalyst deactivation and regeneration, in, Multidisciplinary Digital Publishing Institute, 2015.

VITAE

Name	:	Adeel Ahmad
Nationality	:	Pakistani
Date of Birth	:	12-12-1989
Email	:	adeelahmad677@gmail.com
Telephone	:	+92-3426823253
Address	:	Academic Belt Road, Dhahran 31261, Eastern Province, Kingdom of Saudi Arabia

Academic Background : ***Master of Science***

Chemical Engineering (2020)

King Fahd University of Petroleum and Minerals

Kingdom of Saudi Arabia

Bachelor of Engineering

Chemical Engineering (2013)

University of the Punjab, Lahore

Pakistan